Modelling the residually stressed magneto-electrically coupled soft elastic materials

M.H.B.M. Shariff[1], M. Hossain[2], R. Bustamante[3], J. Merodio[4]

[1] Department of Mathematics
Khalifa University of Science and Technology, UAE.
[2] Zienkiewicz Centre for Computational Engineering, College of Engineering,
Swansea University, Swansea, United Kingdom.
[3] Departamento de Ingeniería Mecánica, Universidad de Chile
Beauchef 851, Santiago Centro, Santiago, Chile.
[4] Department of Continuum Mechanics and Structures, Escuela de Ingenieros de Caminos
Universidad Politecnica de Madrid, 28040 Madrid, Spain

July 14, 2021

Abstract

Residual stresses may exist in different finitely deformed soft multifunctional materials such as in electro-active and magneto-active polymers. In order to develop accurate constitutive frameworks of these smart materials experiencing electro-magneto-mechanically coupled loads, the presence of residual stresses needs to be considered on the onset of the model development. In this contribution, a spectral constitutive equation for finite strain magneto-electric soft material bodies with residual stresses is developed using spectral invariants, where each spectral invariant has a clear physical meaning. A prototype total energy function comprising of single-variable functions is proposed; a single-variable function that depends on an invariant with a direct meaning is easily handled and is experimentally attractive. Results of some boundary value problems are given.

1 Introduction

Multifunctional materials are innovative and smart as they can adapt their physical and mechanical properties as a result of external stimuli. Several external fields can be mentioned including temperature, electric field, magnetic field, humidity, light, pH or combinations of two or more of them [36, 69]. Novel synthesis techniques and experimental characterisations, mathematical modelling, and the search for exotic applications of multifunctional materials have been active fields of research in last two decades. Within the bunch of multifunctional smart materials, the so-called magneto-active polymers (MAPs) and electro-active polymers (EAPs) become widely explored responsive materials thanks to their rapidly-expanding applications in many areas ranging from micro-scale to macro-scale soft robots for targeted drug delivery and for artificial muscles in prosthetics, stretch sensors in monitoring deformations on soft and flexible structures, to mention a few [2, 5, 6, 7, 8, 31, 13, 31, 33, 36, 69]. In the case of EAPs, when an electric voltage will be applied across the thicknesses of system, large deformations will be induced as a result of Coulomb attractions of the opposite charges [31, 33, 41]. In contrast, MAP is a polymeric composite filled with magnetisable particles that can be deformed considerably upon the application of a remotely controlled magnetic field [4, 33]. Both EAPs and MAPs have specific merits and demerits [36]. For instance, EAPs being mostly unfilled polymers, can create huge amount of actuation-driven deformations in contrast to MAPs. However, EAPs require large electrical voltages and demand direct physical contact with the surfaces of an actuated body while for MAPs, no physical attachments between the external field and the systems are required [33, 40, 41]. For an overview of MAPs, a recent review paper by Bastola and Hossain [4] can be consulted.

In MAPs and EAPs, ideally magneto-mechanical and electro-mechanical couplings may occur separately. However, there are some smart materials in which magneto-electrically (ME) coupling may occur simultaneously. In this group, multi-ferroic hard materials will create deformations that can be within small strain ranges. Multi-ferroic ME materials can be applied in the manufacturing of the magneto-electric random access memories (MERAM), see for example [19, 22, 24] for more applications. Nan et al. [45], Pyatakov et al. [49] summarised a wide range of research works and potential usages for ME materials. Note that the early use of magneto-electric materials has been confined to only the area of small-strained hard materials such as ceramics and metals. However, Liu and Sharma [37], Krichen et al. [35] recently proposed an interesting finite strain alternative to small-strained hard MEs. Such a soft polymeric composite can be prepared using all traditional methods used for manufacturing MAPs in which magneto-responsive particles are embedded acting as vehicles for combined magneto-electro-mechanical coupling. Furthermore, Liu et al. [37, 38, 35] mentioned that some living biological matters contain receptors that can be interacted with the presence of magneto field which substantiate the presence of ME coupling effects at finite strains.

Mathematical modelling and simulation of soft materials that can activated under the combined actions of magneto-electro-mechanically coupled field at finite strains is a nascent area [11]. One of the earliest works for fully-coupled thermo-electro-magneto-mechanical multifunctional matters at large strain is due to Santapuri and co-workers [52]. They develop relevant equations in a thermodynamically consistent way that results in an exhaustive list of important quantities of the problems. Very recently, Liu [38] devises the problem of magneto-electro-elasticity based on the principle of minimum free energy. His approach is based on the so-called total free energy function which is applicable to a wide range of multifunctional soft materials starting from electro-magneto-active elastomers to piezo-electric-magnetic materials. Recently, Rambausek and Keip [50] studied the ME coupling in magnetic and electric fields-activated soft composites. They further conclude that the shape effect of fillers is a non-local phenomenon both in EAPs and MAPs. Very recently, Bustamante et al. [11] proposed a modular mathematical structure for modelling magneto-electric soft materials that can finitely be deformed.

Residual stress can be defined as a stress field that exists in an equilibrium system without the application of any external loads or tractions on the boundaries [27]. These stresses are non-homogeneous that result in non-homogeneous responses in a body but their overall response is zero in the system [43, 44]. The existence of residual stresses in living and biological objects such as in plants, human tissues, insects and other animals are very common that may create beneficial or adverse effects [68]. Furthermore, residual stresses may be produced during the manufacturing processes of materials or in geo-mechanics where high stresses can be be developed below the Earth's surface due to the gravitation force. For instance, in the manufacturing of rubberlike materials to be used in bush mountings for the support of engines, residual stresses can be induced during the vulcanisation process [43, 44]. They can also be involved in metal formations or in welded structures. The presence of residual stresses in the multifunctional materials such as MAPs or EAPs might have either beneficial or adverse effects upon the application of subsequent loads [28]. Therefore, such an important aspect needs to be incorporated at the very beginning of the mathematical modelling of these fast growing smart materials.

The origin of residual stresses in EAPs and MAPs could be manifolds. In the case of MAPs, two types of composites are usually manufactured [4]. In the first case, magnetisable particles are more or less homogeneously distributed and locked after the complete curing (solidification) of the mixtures. In contrast, another type of MAPs can be prepared in which particles are arranged towards a particular direction if a magnetic field is applied before the formation of crosslinked chain structures [28, 29]. In both cases, during the transformation of particle-filled composites from a liquid stage to a fully solidified phase, a volume reduction which is frequently termed as the curing-induced volume reduction or shrinkage, may result in residual stresses in MAPs. Very recently, additive manufacturing or 3D printing is widely used for preparing magneto-active polymers in which photo-induced curing techniques are mainly used [36, 69]. Such techniques may also induce differential curing-shrinkage as a result of spatially-oriented light intensity resulting in non-homogeneous residual stresses in MAPs [36]. This can be imagined as an opposite to residual stresses generated in biological tissues as a result of the differential growth [68].

In this contribution, we aim to present a mathematical framework for residually stressed soft polymeric composites that are subjected to electro-magneto-mechanically coupled loads. In the present work we consider as a basis the theory developed recently, see for example references[25, 26, 44, 47, 51], where the residual stress is considered as a variable in the elastic energy of the body along with the deformation gradient, where now in the reference configuration the body is not stress free. We note that the work in references [25, 26] is based on the concept of initial stress symmetry (ISS) and applications of the ISS model can be found in references [14, 15]. The model developed here could be modified to satisfy the ISS model as described in [59], but this modification is beyond the scope of the current paper. We emphasize that the works of [14, 15, 25, 26, 44, 47, 51] uses non-spectral invariants, where most of them do not have clear physical meaning such as the classical invariants (or their variants) given in Spencer [67]; however, in this paper, our proposed formulation uses a set of spectral invariants [53, 55, 56, 59, 60, 62, 64], where each invariant has a clear physical meaning, and hence have an experimental advantage over other types of invariants with no physical interpretation such as the classical invariants [67]. The advantages of spectral invariants over classical invariants are discussed in [65]; hence, we will not elaborate them here. Following our recent work [11] on electro-magnetic-elastic materials, we briefly present the relevant and key governing equations that are essential to represent a magneto-electro-mechanically coupled system at large strains.

2 Preliminaries and governing equations for electro-magneto-mechanically coupled systems

In the absence of an electromagnetic field, we assume, in the undeformed (reference) configuration, the existence of an equilibrium stress field $\boldsymbol{T}_R$ (residual stress) in which the surface traction is zero [64]. The deformation gradient is defined as $\boldsymbol{F} = \dfrac{\partial \boldsymbol{y}}{\partial \boldsymbol{x}}$ in which $\boldsymbol{y}$ and $\boldsymbol{x}$ indicate the vectorial positions of a point in the current and reference configurations, respectively. This is a key quantity in deriving the basic equations for systems that are experiencing the interactions with electro-magnetic fields. For further details, reader is referred to relevant text books, e.g., [20, 34, 39, 42, 48].

2.1 Maxwell equations

In this contribution, the distribution of free charges inside the body is absent. Moreover, there is no electric current in the system. Hence, the Maxwell equations take the form

$$\operatorname{div}\boldsymbol{b} = 0\,, \quad \operatorname{curl}\boldsymbol{e} + \dot{\boldsymbol{b}} = \boldsymbol{0}\,, \quad \operatorname{div}\boldsymbol{d} = 0\,, \quad \operatorname{curl}\boldsymbol{h} = \dot{\boldsymbol{d}}\,, \quad \boldsymbol{d} = \varepsilon_0\boldsymbol{e} + \boldsymbol{p}\,, \quad \boldsymbol{b} = \mu_0(\boldsymbol{h} + \boldsymbol{m})\,, \tag{1}$$

where $\boldsymbol{b}$ is the magnetic induction, $\boldsymbol{e}$ is the electric field, $\boldsymbol{d}$ is the electric displacement, $\boldsymbol{h}$ is the magnetic field, $\boldsymbol{p}$ is the electric polarization, $\boldsymbol{m}$ is the magnetization, ε_0 is the electric permittivity in vacuum, μ_0 is the magnetic permeability in vacuum, div and curl are, respectively, the divergence and curl of a vector with respect to $\boldsymbol{y}$ and $\dot{()}$ is the time derivative at fixed $\boldsymbol{y}$ The first law of motion is

$$\boldsymbol{f}_b + \boldsymbol{f}_e = \rho\boldsymbol{a}_a - \operatorname{div}\boldsymbol{T}_C\,, \tag{2}$$

where $\boldsymbol{a}_a$ is the acceleration, ρ is the density in the current configuration, $\boldsymbol{T}_C$ is the Cauchy stress , $\boldsymbol{f}_b$ is the body force independent of electromagnetic fields and [48]

$$\boldsymbol{f}_e = (\operatorname{grad}\boldsymbol{e})^T\boldsymbol{p} + (\operatorname{grad}\boldsymbol{b})^T\boldsymbol{m} + \dot{\overline{\boldsymbol{p}\times\boldsymbol{b}}} + \operatorname{div}[\boldsymbol{v}\otimes(\boldsymbol{p}\times\boldsymbol{b})]\,, \tag{3}$$

where $\otimes$ denotes the dyadic product. The Lagrangian magnetic and electric variables are defined as [11, 12]

$$\boldsymbol{b}_L = J\boldsymbol{F}^{-1}\boldsymbol{b}\,, \quad \boldsymbol{e}_l = \boldsymbol{F}^T\boldsymbol{e}\,, \tag{4}$$

where $J = \det\boldsymbol{F}$ and $\det$ denotes the determinant of a tensor. Using the relations (see Appendix A)

$$\operatorname{div}[\boldsymbol{d}\otimes\boldsymbol{e} - \frac{1}{2}\varepsilon_0(\boldsymbol{e}\cdot\boldsymbol{e})\boldsymbol{I}] = (\operatorname{curl}\boldsymbol{e})\times\boldsymbol{p} + (\operatorname{grad}\boldsymbol{e})^T\boldsymbol{p} + \varepsilon_0(\operatorname{curl}\boldsymbol{e})\times\boldsymbol{e}\,, \tag{5}$$

we have in view of (1)

$$(\operatorname{grad}\boldsymbol{e})^T\boldsymbol{p} = \operatorname{div}[\boldsymbol{d}\otimes\boldsymbol{e} - \frac{1}{2}\varepsilon_0(\boldsymbol{e}\cdot\boldsymbol{e})\boldsymbol{I}] + \dot{\boldsymbol{b}}\times\boldsymbol{d}\,. \tag{6}$$

Using the relations

$$\frac{1}{\mu_0}\operatorname{div}[\boldsymbol{b}\otimes\boldsymbol{b} - \frac{1}{2}(\boldsymbol{b}\cdot\boldsymbol{b})\boldsymbol{I}] = \frac{1}{\mu_0}(\operatorname{curl}\boldsymbol{b})\times\boldsymbol{b} = \dot{\boldsymbol{d}}\times\boldsymbol{b} + (\operatorname{curl}\boldsymbol{m})\times\boldsymbol{b} \tag{7}$$

and

$$\operatorname{div}[(\boldsymbol{m}\cdot\boldsymbol{b})\boldsymbol{I}-\boldsymbol{b}\otimes\boldsymbol{m}]=(\operatorname{grad}\boldsymbol{b})^T\boldsymbol{m}-(\operatorname{curl}\boldsymbol{m})\times\boldsymbol{b}\,, \tag{8}$$

we have

$$(\operatorname{grad}\boldsymbol{b})^T\boldsymbol{m}=\operatorname{div}\left[\frac{1}{\mu_0}(\boldsymbol{b}\otimes\boldsymbol{b}-\frac{1}{2}(\boldsymbol{b}\cdot\boldsymbol{b})\boldsymbol{I})+(\boldsymbol{m}\cdot\boldsymbol{b})\boldsymbol{I}-\boldsymbol{b}\otimes\boldsymbol{m}\right]-\dot{\boldsymbol{d}}\times\boldsymbol{b}\,. \tag{9}$$

Following the works of [9, 62, 64], the free energy is assumed to take the form

$$\rho\psi(\boldsymbol{F},\boldsymbol{T}_R,\boldsymbol{b},\boldsymbol{e}^e)=\rho\psi(\boldsymbol{F},\boldsymbol{T}_R,\frac{1}{J}\boldsymbol{F}\boldsymbol{b}_L,\boldsymbol{F}^{-T}\boldsymbol{e}^e_L)=W_{(a)}(\boldsymbol{U},\boldsymbol{T}_R,\boldsymbol{b}_L,\boldsymbol{e}^e_L)\,, \tag{10}$$

where

$$\boldsymbol{e}^e=\boldsymbol{e}+\boldsymbol{v}\times\boldsymbol{b}\,,\quad \boldsymbol{e}^e_L=\boldsymbol{F}^T\boldsymbol{e}^e \tag{11}$$

$\boldsymbol{v}$ is the velocity and $\boldsymbol{U}$ is the right stretch tensor. In view of the Second Law of Thermodynamics [9], we obtain

$$\boldsymbol{T}_C\boldsymbol{F}^{-T}=\rho\frac{\partial\psi}{\partial\boldsymbol{F}}\,,\quad \boldsymbol{p}=-\rho\frac{\partial\psi}{\partial\boldsymbol{e}^e}\,,\quad \boldsymbol{m}_e=-\rho\frac{\partial\psi}{\partial\boldsymbol{b}}\,, \tag{12}$$

where

$$\boldsymbol{m}_e=\boldsymbol{m}+\bar{\boldsymbol{m}}\,,\quad \bar{\boldsymbol{m}}=\boldsymbol{v}\times\boldsymbol{p}\,. \tag{13}$$

In view of the relations in (10), (12) and the formulae

$$\frac{\partial\boldsymbol{e}^e}{\partial\boldsymbol{F}}=-\boldsymbol{F}^{-T}\otimes\boldsymbol{e}^e\,,\quad \frac{\partial\boldsymbol{b}}{\partial\boldsymbol{F}}=\frac{1}{J}[-\boldsymbol{F}\boldsymbol{b}_L\otimes\boldsymbol{F}^{-1}+\sum_{i=1}^{3}\boldsymbol{g}_i\otimes\boldsymbol{b}_L\otimes\boldsymbol{g}_i]\,, \tag{14}$$

where $\{\boldsymbol{g}_1,\boldsymbol{g}_2,\boldsymbol{g}_3\}$ is a Cartesian basis, the Cauchy stress then takes the form

$$\boldsymbol{T}_C=\rho\boldsymbol{F}\frac{\partial\psi}{\partial\boldsymbol{F}}=2\boldsymbol{F}\frac{\partial W_{(a)}}{\partial\boldsymbol{C}}\boldsymbol{F}^T-\boldsymbol{p}\otimes\boldsymbol{e}-(\boldsymbol{m}_e\cdot\boldsymbol{b})\boldsymbol{I}+\boldsymbol{b}\otimes\boldsymbol{m}_e\,. \tag{15}$$

The equation of motion (2) also takes the form

$$\begin{aligned}\rho\boldsymbol{a}_a=\operatorname{div}\left\{2\boldsymbol{F}\frac{\partial W_{(a)}}{\partial\boldsymbol{C}}\boldsymbol{F}^T+\frac{1}{\mu_0}[\boldsymbol{b}\otimes\boldsymbol{b}-\frac{1}{2}(\boldsymbol{b}\cdot\boldsymbol{b})\boldsymbol{I}]+\varepsilon_0[\boldsymbol{e}\otimes\boldsymbol{e}-\frac{1}{2}(\boldsymbol{e}\cdot\boldsymbol{e})\boldsymbol{I}]+\boldsymbol{p}\otimes(\boldsymbol{v}\times\boldsymbol{b})\right\}\\ +\dot{\overline{\boldsymbol{p}\times\boldsymbol{b}}}+\dot{\boldsymbol{b}}\times(\boldsymbol{b}-\boldsymbol{d})+\boldsymbol{f}\,.\end{aligned} \tag{16}$$

The above expression makes use of the relation

$$\boldsymbol{p}\otimes(\boldsymbol{v}\times\boldsymbol{b})=\boldsymbol{b}\otimes\bar{\boldsymbol{m}}-(\bar{\boldsymbol{m}}\cdot\boldsymbol{b})\boldsymbol{I}+\boldsymbol{v}\otimes(\boldsymbol{p}\times\boldsymbol{b})\,. \tag{17}$$

Introducing a *symmetric stress-like* tensor

$$\boldsymbol{T}_T = 2\boldsymbol{F}\frac{\partial W_{(a)}}{\partial \boldsymbol{C}}\boldsymbol{F}^T + \frac{1}{\mu_0}[\boldsymbol{b}\otimes\boldsymbol{b} - \frac{1}{2}(\boldsymbol{b}\cdot\boldsymbol{b})\boldsymbol{I}] + \varepsilon_0[\boldsymbol{e}\otimes\boldsymbol{e} - \frac{1}{2}(\boldsymbol{e}\cdot\boldsymbol{e})\boldsymbol{I}]\,, \tag{18}$$

we have the simplified equation of motion

$$\rho\boldsymbol{a}_a = \mathrm{div}\,[\boldsymbol{T}_T + \boldsymbol{p}\otimes(\boldsymbol{v}\times\boldsymbol{b})] + \dot{\overline{\boldsymbol{p}\times\boldsymbol{b}}} + \dot{\boldsymbol{b}}\times(\boldsymbol{b}-\boldsymbol{d}) + \boldsymbol{f}_b\,. \tag{19}$$

In view of (15), the equilibrium of moments [48]

$$\boldsymbol{E}_A\boldsymbol{T}_C = \boldsymbol{p}\times\boldsymbol{e} + \boldsymbol{m}_e\times\boldsymbol{b} \tag{20}$$

is satisfied, where $\boldsymbol{E}_A$ is the permutation tensor and the operation

$$\boldsymbol{E}_A(\boldsymbol{a}\otimes\boldsymbol{c}) = \boldsymbol{c}\times\boldsymbol{a} \tag{21}$$

is used to obtain (20); $\boldsymbol{a}$ and $\boldsymbol{c}$ are vectors.

Note that in the time-independent case, the stress like tensor $\boldsymbol{T}_T$ becomes the *total stress* tensor and we have

$$\mathrm{div}\boldsymbol{T}_T + \boldsymbol{f} = \boldsymbol{0}\,, \tag{22}$$

taking note that, in this case, $W_{(a)}(\boldsymbol{U},\boldsymbol{T}_R,\boldsymbol{b}_L,\boldsymbol{e}_L^e)$ becomes $W_{(a)}(\boldsymbol{U},\boldsymbol{T}_R,\boldsymbol{b}_L,\boldsymbol{e}_L)$.

Following the work of [11], we can express

$$J\boldsymbol{T}_T = 2\boldsymbol{F}\frac{\partial\Omega}{\partial\boldsymbol{C}}\boldsymbol{F}^T\,, \tag{23}$$

where the total energy

$$\Omega = W_{(a)}(\boldsymbol{U},\boldsymbol{T}_R,\boldsymbol{b}_L,\boldsymbol{e}_L) + W_{(b)}(\boldsymbol{U},\boldsymbol{b}_L,\boldsymbol{e}_L)\,, \tag{24}$$

$$W_{(b)}(\boldsymbol{U},\boldsymbol{b}_L,\boldsymbol{e}_L) = \frac{1}{2J\mu_0}\boldsymbol{b}_L\cdot\boldsymbol{C}\boldsymbol{b}_L - \frac{J\varepsilon_0}{2}\boldsymbol{e}_L\cdot\boldsymbol{C}^{-1}\boldsymbol{e}_L\,. \tag{25}$$

If the incompressibility assumption $J=1$ is activated, we have the relations

$$\boldsymbol{T}_T = 2\boldsymbol{F}\frac{\partial\Omega}{\partial\boldsymbol{C}}\boldsymbol{F}^T - p\boldsymbol{I}\,, \tag{26}$$

where p is the Lagrange multiplier due to the incompressible constraint.

In this paper, we only focus on time-independent problems and incompressible materials. Hence, we have,

$$\mathrm{div}\,\boldsymbol{b} = 0\,,\quad \mathrm{curl}\,\boldsymbol{e} = \boldsymbol{0}\,,\quad \mathrm{div}\,\boldsymbol{d} = 0\,,\quad \mathrm{curl}\,\boldsymbol{h} = \boldsymbol{0}\,. \tag{27}$$

The Lagrangian results

$$\mathrm{Div}\,\boldsymbol{b}_L = 0\,,\quad \mathrm{Curl}\,\boldsymbol{e}_L = \boldsymbol{0}\,,\quad \mathrm{Div}\,\boldsymbol{d}_L = 0\,,\quad \mathrm{Curl}\,\boldsymbol{h}_L = \boldsymbol{0}\,, \tag{28}$$

where

$$
\boldsymbol{d}_L = -\frac{\partial \Omega}{\partial \boldsymbol{e}_L}\,, \quad \boldsymbol{h}_L = \frac{\partial \Omega}{\partial \boldsymbol{b}_L}\,, \tag{29}
$$

are obtained in [10]: Div and Curl are, respectively, the divergence and curl of a vector with respect to $\boldsymbol{x}$ and

$$
\boldsymbol{d}_L = \boldsymbol{F}^{-1}\boldsymbol{d}\,, \quad \boldsymbol{h}_L = \boldsymbol{F}^T\boldsymbol{h} \tag{30}
$$

In view of $(27)_{2,4}$ and $(28)_{2,4}$, we could write

$$
\boldsymbol{e} = \frac{\partial \Psi_e}{\partial \boldsymbol{y}}\,, \quad \boldsymbol{h} = \frac{\partial \Psi_h}{\partial \boldsymbol{y}}\,, \quad \boldsymbol{e}_L = \frac{\partial \Psi_E}{\partial \boldsymbol{x}}\,, \quad \boldsymbol{h}_L = \frac{\partial \Psi_H}{\partial \boldsymbol{x}}\,, \tag{31}
$$

where Ψ_e, Ψ_h, Ψ_E and Ψ_H are scalar functions.

In vaccum, the Maxwell stress tensor $\boldsymbol{T}_M$ outside the body is given by

$$
\boldsymbol{T}_{\mathrm{M}} = \boldsymbol{d}\otimes\boldsymbol{e} + \boldsymbol{h}\otimes\boldsymbol{b} - \frac{1}{2}[\boldsymbol{d}\cdot\boldsymbol{e} + \boldsymbol{h}\cdot\boldsymbol{b}]\boldsymbol{I} = \varepsilon_0(\boldsymbol{e}\otimes\boldsymbol{e} - \frac{\boldsymbol{e}\cdot\boldsymbol{e}}{2}\boldsymbol{I}) + \frac{1}{\mu_0}(\boldsymbol{b}\otimes\boldsymbol{b} - \frac{\boldsymbol{b}\cdot\boldsymbol{b}}{2}\boldsymbol{I})\,. \tag{32}
$$

The continuity equations for the electromagnetic variables $\boldsymbol{b}$, $\boldsymbol{h}$, $\boldsymbol{d}$, $\boldsymbol{e}$ and the total stress $\boldsymbol{T}_T$ are given in reference [11]. Electromagnetic theory details can be found from, for example, in [34, 39, 42, 48].

3 Spectral constitutive equation: Time independent processes

In view of (24), we can express Ω via the variables

$$
\boldsymbol{U}, \quad \boldsymbol{T}_R, \quad \boldsymbol{f}, \quad \boldsymbol{g}\,, \quad b_L, \quad e_L\,, \tag{33}
$$

where $\boldsymbol{f}$ and $\boldsymbol{g}$ are unit vectors and

$$
\boldsymbol{b}_L = b_L\boldsymbol{f}\,, \quad \boldsymbol{e}_L = e_L\boldsymbol{g}\,, \quad b_L = \sqrt{\boldsymbol{b}_L\cdot\boldsymbol{b}_L}\,, \quad e_L = \sqrt{\boldsymbol{e}_L\cdot\boldsymbol{e}_L}\,. \tag{34}
$$

Ω must be form invariant with respect to any rotation $\boldsymbol{Q}$ at the reference configuration, i.e.,

$$
\Omega(\boldsymbol{U}, \boldsymbol{T}_R, \boldsymbol{f}, \boldsymbol{g}, b_L, e_L) = \Omega(\boldsymbol{Q}\boldsymbol{U}\boldsymbol{Q}^T, \boldsymbol{Q}\boldsymbol{T}_R\boldsymbol{Q}^T, \boldsymbol{Q}\boldsymbol{f}, \boldsymbol{Q}\boldsymbol{g}, b_L, e_L)\,. \tag{35}
$$

Hence, we can express Ω in terms of the isotropic invariants of the set $S = \{\boldsymbol{U}, \boldsymbol{T}_R, \boldsymbol{b}_L, \boldsymbol{e}_L\}$. To obtain these isotropic invariants, following the work of Shariff et al. [64], we simply express the components of the elements of S using the basis $\{\boldsymbol{u}_1, \boldsymbol{u}_2, \boldsymbol{u}_3\}$, where the unit vector $\boldsymbol{u}_i$ is an eigenvector of

$$
\boldsymbol{U} = \sum_{i=1}^{3} \lambda_i \boldsymbol{u}_i \otimes \boldsymbol{u}_i\,. \tag{36}
$$

Accordingly, we can express Ω in terms of the spectral component invariants

$$
\begin{aligned}
&\lambda_i = \boldsymbol{u}_i\cdot\boldsymbol{U}\boldsymbol{u}_i = \boldsymbol{Q}\boldsymbol{u}_i\cdot\boldsymbol{Q}\boldsymbol{U}\boldsymbol{Q}^T\boldsymbol{Q}\boldsymbol{u}_i\,, \quad f_i = \boldsymbol{u}_i\cdot\boldsymbol{f} = \boldsymbol{Q}\boldsymbol{u}_i\cdot\boldsymbol{Q}\boldsymbol{f}\,, \quad g_i = \boldsymbol{u}_i\cdot\boldsymbol{g} = \boldsymbol{Q}\boldsymbol{u}_i\cdot\boldsymbol{Q}\boldsymbol{g}\,,\\
&t_{ij} = \boldsymbol{u}_i\cdot\boldsymbol{T}_R\boldsymbol{u}_j = \boldsymbol{Q}\boldsymbol{u}_i\cdot\boldsymbol{Q}\boldsymbol{T}_R\boldsymbol{Q}^T\boldsymbol{Q}\boldsymbol{u}_j\,, \quad e_L\,, \quad b_L\,.
\end{aligned} \tag{37}
$$

We must emphasize that the components of the vectors and tensors in the set S, with respect to an *arbitrary* basis, are not, in general, invariants. Since $\boldsymbol{f}$ and $\boldsymbol{g}$ are unit vectors, we have,

$$\sum_{i=1}^{3} f_i^2 = 1\,, \quad \sum_{i=1}^{3} g_i^2 = 1\,, \tag{38}$$

hence, only 15 of the 17 invariants in (37) are independent [58, 66]. The set of 17 invariants in (37) can be considered to be an irreducible functional basis [54, 66], since *all* invariants for the set S can be explicitly expressed in terms of the spectral invariants in (37). We strongly point out that all 37 classical invariants in the minimal integrity basis [67] for the set of tensors S can be explicitly expressed in terms of the spectral invariants given in (37). For example, the minimal integrity classical invariant

$$\text{tr}\ (\boldsymbol{b}_L \otimes \boldsymbol{b}_L \boldsymbol{C}\boldsymbol{T}_R) = \boldsymbol{b}_L \cdot (\boldsymbol{C}\boldsymbol{T}_R \boldsymbol{b}_L) = \sum_{i,j} b_L^2 f_i f_j \lambda_j^2 t_{ij}\,, \tag{39}$$

which clearly shows that it can be expressed in terms of the spectral invariants (37). Relations between Spencer [67] classical invariants and spectral invariants can be found in Shariff [66], where he has shown that only 13 (if we ignore b_L and e_L) of the 37 classical invariants in the minimal integrity basis for the set S are independent. If we consider the positive and negative values of f_i and g_i as distinct single-valued functions, in view of (38), then the number of invariants in the irreducible functional basis is reduced to 15. Advantages of spectral invariants over classical invariants are discussed, for example, in reference [65].

For convenience, we express

$$\Omega = W(\boldsymbol{U}, \boldsymbol{T}_R, \boldsymbol{f}, \boldsymbol{g}, b_L, e_L) + \frac{b_L^2}{2J\mu_0} \sum_{i=1}^{3} \beta_i \lambda_i^2 - \frac{J\varepsilon_0 e_L^2}{2} \sum_{i=1}^{3} \frac{\gamma_i}{\lambda_i^2}\,, \tag{40}$$

where

$$\beta_i = f_i^2\,, \quad \gamma_i = g_i^2\,. \tag{41}$$

Ω is required to satisfy the P-property [55] and to assist this requirement, the independent invariants

$$\zeta_i = t_{ii} = \boldsymbol{u}_i \cdot \boldsymbol{T}_R \boldsymbol{u}_i\,, \quad \chi_i = \boldsymbol{u}_i \cdot \boldsymbol{T}_R^2 \boldsymbol{u}_i \tag{42}$$

are used in Ω (instead of the invariants t_{ij}).

In view of (23), we require the Lagrangian spectral components of the derivative $\dfrac{\partial \Omega}{\partial \boldsymbol{C}}$ [60] i.e.,

$$\left(\frac{\partial \Omega}{\partial \boldsymbol{C}}\right)_{ii} = \frac{1}{2\lambda_i} \frac{\partial \Omega}{\partial \lambda_i}\,, \tag{43}$$

$$\left(\frac{\partial \Omega}{\partial \boldsymbol{C}}\right)_{ij} = \frac{\dfrac{\partial \Omega}{\partial \boldsymbol{u}_i} \cdot \boldsymbol{u}_j - \dfrac{\partial \Omega}{\partial \boldsymbol{u}_j} \cdot \boldsymbol{u}_i}{2(\lambda_i^2 - \lambda_j^2)}\,, \quad i \neq j\,. \tag{44}$$

In view of (28), we also require the Lagrangian relations

$$\frac{\partial \Omega}{\partial \boldsymbol{b}_L} = \frac{\partial \Omega}{\partial b_L}\boldsymbol{f} + \frac{1}{b_L}\left[(\boldsymbol{I} - \boldsymbol{f}\otimes\boldsymbol{f})^T \frac{\partial \Omega}{\partial \boldsymbol{f}}\right] , \tag{45}$$

$$\frac{\partial \Omega}{\partial \boldsymbol{e}_L} = \frac{\partial \Omega}{\partial e_L}\boldsymbol{g} + \frac{1}{e_L}\left[(\boldsymbol{I} - \boldsymbol{g}\otimes\boldsymbol{g})^T \frac{\partial \Omega}{\partial \boldsymbol{g}}\right] . \tag{46}$$

If we express the total stress in terms of the Eulerian basis $\{\boldsymbol{v}_1, \boldsymbol{v}_2, \boldsymbol{v}_3\}$, we have

$$\boldsymbol{T}_T = \sum_{i,j=1}^{3} \tau_{ij}\boldsymbol{v}_i \otimes \boldsymbol{v}_j , \tag{47}$$

where

$$\tau_{ii} = \lambda_i \frac{\partial \Omega}{\partial \lambda_i} - p , \quad i \quad \text{not summed} , \tag{48}$$

$$\begin{aligned} \tau_{ij} \; = \; & \frac{2\lambda_i\lambda_j}{\lambda_i^2 - \lambda_j^2}\left[(\frac{\partial \Omega}{\partial \beta_i} - \frac{\partial \Omega}{\partial \beta_j})f_i f_j + (\frac{\partial \Omega}{\partial \gamma_i} - \frac{\partial \Omega}{\partial \gamma_j})g_i g_j + (\frac{\partial \Omega}{\partial \zeta_i} - \frac{\partial \Omega}{\partial \zeta_j})t_{ij} \right. \\ & + \left. (\frac{\partial \Omega}{\partial \chi_i} - \frac{\partial \Omega}{\partial \chi_j})\boldsymbol{u}_i \boldsymbol{T}_R^2 \boldsymbol{u}_j\right] , \quad i \neq j , \end{aligned} \tag{49}$$

$\boldsymbol{v}_i = \boldsymbol{R}\boldsymbol{u}_i$ and $\boldsymbol{R} = \boldsymbol{F}\boldsymbol{U}^{-1}$.

4 Boundary value problems

Until now there is no experimental data available in the literature to propose any meaningful specific expressions for Ω that could fit and predict experimental data. However, in order to plot graphs and have some discussion on the the anisotropic mechanical behavior, the influence of residual stress, magnetic and electric fields on elastic solids, at least a prototype for Ω has to be proposed. The proposed prototype given below is simple in form, but without experimental data to evaluate its performances, it may or may not be a good candidate to represent the elastic solids that are considered in this paper. A finite strain constitutive equation that is consistent with the general theory of infinitesimal elasticity and contains couplings between residual stress, electric and magnetic fields requires numerous material constants and invariant functions (see for example references [59, 64]). Illustration of the theory would be far too complicated if all such material constants and invariant functions were to be included. However, for the application considered in the following sections, a considerably reduced set of material constants and invariant functions will be adopted. We strongly emphasize that, except for the invariants χ_i, all the spectral invariants are included in the simple prototype for Ω, proposed below. Using the same concept described in references [59, 64], coupling terms, if required, could be easily inserted in the simple prototype given in (50), below.

Only quasi-static deformations are considered. At the outset, cylindrical results for simple tension, extension and inflation of a thicked- wall tube, simple torsion and, extension, inflation and torsion of a thick-walled cylindrical tube are given. Later, we obtain results for an equibiaxial deformation applied on a thin sheet of material. We note that, up to our current knowledge, we believe that there are no experimental data on residually stressed electro-magneto solids to validate our theory. However, the results obtained in this Section can be experimentally useful, where they could be used to compare with future experimental data.

In order to illustrate the effects of residual stresses on electro-magneto-active solids, we require a specific form for Ω. Based on the work of Shariff [56, 62, 64] we propose a prototype

$$\Omega = W_R + N_1 + N_2 + \frac{b_L^2}{2\mu_0}\sum_{i=1}^{3}\beta_i\lambda_i^2 - \frac{\epsilon_0 e_L^2}{2}\sum_{i=1}^{3}\frac{\gamma_i}{\lambda_i^2}\,, \tag{50}$$

where

$$W_R = \sum_{i=1}^{3}\left\{\mu r_1(\lambda_i) + \zeta_i r_2(\lambda_i)\right\}\,, \tag{51}$$

$\mu > 0$ (see, for example, Ref. [53]) is a material parameter,

$$N_1 = c_0(e_L)\sum_{i=1}^{3}\gamma_i r_3(\lambda_i)\,, \quad N_2 = c_1(b_L)\sum_{i=1}^{3}\beta_i r_4(\lambda_i)\,, \tag{52}$$

c_0 and c_1 are functions of e_L and b_L, respectively. The conditions

$$\begin{aligned} &r_1(1) = r_2(1) = r_3(1) = r_4(1) = r_1'(1) = r_3'(1) = r_4'(1) = 0\,,\\ &r_1''(1) = r_3''(1) = r_4''(1) = 2\,, \quad r_2'(1) = 1 \end{aligned} \tag{53}$$

are required to ensure that Ω is consistent with the theory infinitesimal elasticity. For $|\ \lambda_i - 1\ | << 1$, r_1, r_3, r_4 are approximately quadratic in $\lambda_i - 1$ and r_2 is linear in $\lambda_i - 1$. Extending these behaviours to finite strain, the conditions

$$r_1(x), r_3(x), r_4(x) \geq 0\,, \quad x > 0\,, \quad r_2(x) \geq 0 \quad x \geq 1\,, \quad r_2(x) < 0\,, \quad 0 < x < 1 \tag{54}$$

are suggested. Note that r_1', r_3', r_4' and r_2 are monotically increasing functions. The above simple form (51) is a generalization of previous prototypes, for example, Jha et al. [32] proposed, for an incompressible body, the prototype

$$\begin{aligned} W_R &= \frac{\mu}{2}(I_1 - 3) + \frac{f}{2}(I_5 - \mathrm{tr}\boldsymbol{T}_R) + \frac{1-f}{4}(I_6 - \mathrm{tr}\boldsymbol{T}_R)\\ &= \frac{\mu}{2}(I_1 - 3 - 2\ln J) + \frac{f}{2}(I_5 - \mathrm{tr}\boldsymbol{T}_R) + \frac{1-f}{4}(I_6 - \mathrm{tr}\boldsymbol{T}_r)\,, \quad 0 \leq f \leq 1\,, \end{aligned} \tag{55}$$

where $I_1 = \mathrm{tr}\boldsymbol{C}$, $I_5 = \mathrm{tr}(\boldsymbol{T}_R\boldsymbol{C})$, $I_6 = \mathrm{tr}(\boldsymbol{T}_R\boldsymbol{C}^2)$ and $J = 1$. In this case, we simply have

$$r_1(x) = \frac{x^2 - 2\ln x - 1}{2}\,, \quad r_2(x) = \frac{f}{2}(x^2 - 1) + \frac{1-f}{4}(x^4 - 1)\,. \tag{56}$$

In the undeformed configuration ($\boldsymbol{F} = \boldsymbol{I}$) with no electro-magnetic fields, in view of the properties given in (53), Eqn. (26) becomes

$$\boldsymbol{T}_R = -p_0\boldsymbol{I} + \boldsymbol{T}_R\,, \tag{57}$$

which implies that $p_0 = 0$; p_0 is the value of p in the reference configuration (i.e. at $\boldsymbol{F} = \boldsymbol{I}$).

From (45), (46), (50) and (52), it is clear that

$$\boldsymbol{d} = \epsilon_0 \boldsymbol{e} - \boldsymbol{F}\frac{\partial N_1}{\partial \boldsymbol{e}_L}\,, \quad \boldsymbol{p} = -\boldsymbol{F}\frac{\partial N_1}{\partial \boldsymbol{e}_L} \tag{58}$$

and

$$\boldsymbol{b} = \mu_0[\boldsymbol{h} - \boldsymbol{F}^{-T}\frac{\partial N_2}{\partial \boldsymbol{b}_L}]\,, \quad \boldsymbol{m} = -\boldsymbol{F}^{-T}\frac{\partial N_2}{\partial \boldsymbol{b}_L}\,. \tag{59}$$

In vacuum $N_1 = N_2 = 0$ and we recover the relations

$$\boldsymbol{d} = \epsilon_0 \boldsymbol{e}\,, \quad \boldsymbol{b} = \mu_0 \boldsymbol{h}\,. \tag{60}$$

Ground-state-constant constraints for Ω are obtained via the strong ellipticity condition. In this paper, we will not derive the general inequalities required for the ground-state constants of the total energy function (50). Since in this section, we deal with problems that can be considered as two dimensional, we will give some inequality results for $\mathbf{m}$ and $\mathbf{n}$ in a plane and assume $\boldsymbol{T}_R = t_1\mathbf{d}_1 \otimes \mathbf{d}_1 + t_2\mathbf{d}_2 \otimes \mathbf{d}_2$ in that plane, where t_1, t_2 and $\boldsymbol{d}_1, \boldsymbol{d}_2$ are, respectively, the eigenvalues and eigenvectors of $\boldsymbol{T}_R$. Based on the work of [64], the necessary and sufficient conditions to satisfy the (two-dimensional) strong ellipticity condition are

$$b_1 > 0 \quad \text{and} \quad 4b_1b_2 > b_3\,, \tag{61}$$

where

$$\begin{aligned}
b_1 &= \mu + \frac{r_2''(1)}{4}(t_1+t_2) + \frac{1}{4}(3t_1 - t_2) + \frac{c_0(e_L)}{2}(g_1^2+g_2^2) + \frac{c_1(b_L)}{2}(f_1^2+f_2^2) - \epsilon_0 e_L^2 g_2^2 + \frac{b_L^2}{\mu_o}f_1^2\,,\\
b_2 &= \mu + \frac{r_2''(1)}{4}(t_1+t_2) + \frac{1}{4}(3t_2 - t_1) + \frac{c_0(e_L)}{2}(g_1^2+g_2^2) + \frac{c_1(b_L)}{2}(f_1^2+f_2^2) - \epsilon_0 e_L^2 g_1^2 + \frac{b_L^2}{\mu_o}f_2^2\,,\\
b_3 &= 2\epsilon_0 e_L^2 g_1 g_2 + \frac{b_L^2}{\mu_o}f_1 f_2\,,
\end{aligned} \tag{62}$$

taking note that, since the basis $\{\boldsymbol{u}_1, \boldsymbol{u}_2, \boldsymbol{u}_3\}$ is arbitrary in the reference configuration ($\boldsymbol{F}$=$\boldsymbol{I}$), we could equate $\boldsymbol{d}_i = \boldsymbol{u}_i$.

We make it clear that we are not interested in constructing the optimal forms of $r_1 \ldots r_4$ for a particular material in this paper. Their optimal forms for a particular material require rigourous analyses (such as those given in Shariff [53, 61]), which is outside the scope of this paper. However, to plot the graphs in the boundary value problems below, we simply use the functions and constant values

$$r_1(x) = (\ln(x))^2\,, \quad r_2(x) = x - 1\,, \quad r_3(x) = r_4(x) = (x-1)^2\,, \tag{63}$$

$$\mu = 10\,\text{kPa}\,, \quad c_0(e_L) = 0.1\epsilon_0 e_L^2\,, \quad c_1(b_L) = \frac{b_L^2}{0.01\mu_0} \tag{64}$$

with the standard values

$$\epsilon_0 = 8.85 \times 10^{-12}\ \text{F/m}, \quad \mu_0 = 4\pi \times 10^{-7}\ \text{H/m}\,. \tag{65}$$

and in the figures below $\eta = \sqrt{1000}$.

4.1 Cylindrical problems

4.1.1 Cylindrical problems containing residual stresses

For cylindrical problems, we consider a geometry of a circular cylindrical tube defined by

$$A \leq R \leq B, \quad 0 \leq \Theta \leq 2\pi, \quad 0 \leq Z \leq L\,, \tag{66}$$

where (R, Θ, Z) is the referential cylindrical polar coordinate.

For the purpose of obtaining results in sections 4.1.2 to 4.1.5, we consider the residual stress field that is similar to that described in [62], i.e.,

$$\boldsymbol{T}_R = t_1(R)\boldsymbol{E}_R \otimes \boldsymbol{E}_R + t_2(R)\boldsymbol{E}_\Theta \otimes \boldsymbol{E}_\Theta\,, \tag{67}$$

where $\boldsymbol{E}_R$, $\boldsymbol{E}_\Theta$ and $\boldsymbol{E}_Z$ referential cylindrical polar vectors,

$$t_1 = \frac{\kappa}{B^2}(R-A)(R-B)\,, \quad t_2 = \frac{\kappa}{B^2}(3R^2 - 2(A+B)R + AB) \tag{68}$$

and κ is a constant and has the same dimension as stress. The residual stress (67) satisfies the equilibrium equation

$$\frac{dt_1}{dR} + \frac{1}{R}(t_1 - t_2) = 0 \tag{69}$$

and stress free surface in the reference frame.

In sections 4.1.2 to 4.1.5, all tensor and vector components are cylindrical polar components.

4.1.2 Simple Tension

When a cylinder with $A = 0$ experiences uniform extension, it can be expressed as,

$$r = \frac{1}{\sqrt{\lambda_z}}R\,, \quad \theta = \Theta\,, \quad z = \lambda_z Z\,. \tag{70}$$

Note that (r, θ, z) is the current configuration polar coordinate and

$$\boldsymbol{F} = \frac{1}{\sqrt{\lambda_z}}\boldsymbol{e}_r \otimes \boldsymbol{E}_R + \frac{1}{\sqrt{\lambda_z}}\boldsymbol{e}_\theta \otimes \boldsymbol{E}_\Theta + \lambda_z \boldsymbol{e}_z \otimes \boldsymbol{E}_Z\,, \tag{71}$$

where $\lambda_1 = \lambda_r = \dfrac{1}{\sqrt{\lambda_z}}, \lambda_2 = \lambda_r = \dfrac{1}{\sqrt{\lambda_z}}\,, \lambda_3 = \lambda_z$. Here, the vectors $\boldsymbol{e}_r$, $\boldsymbol{e}_\theta$ and $\boldsymbol{e}_z$ are cylindrical polar coordinate vectors associated with the deformed configuration. For simplicity, we only consider the magnetic induction and the electric field to be

$$\boldsymbol{b} = B_0\boldsymbol{e}_z\,, \quad \boldsymbol{e} = E_0\boldsymbol{e}_z\,. \tag{72}$$

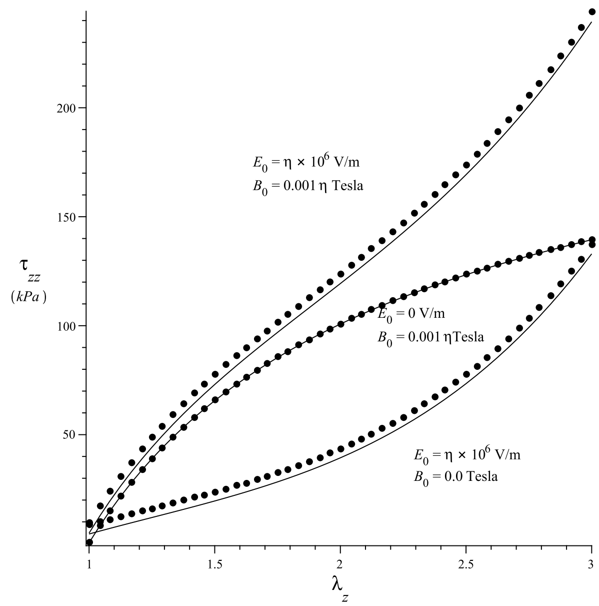

Figure 1: Axial stress τ_{zz} vs λ_z for various values of E_0 and B_0. Points represent zero surface traction. Lines represent surface traction equals to $(\boldsymbol{T}_M)_{rr}$. Axial stress is independent of the residual stress.

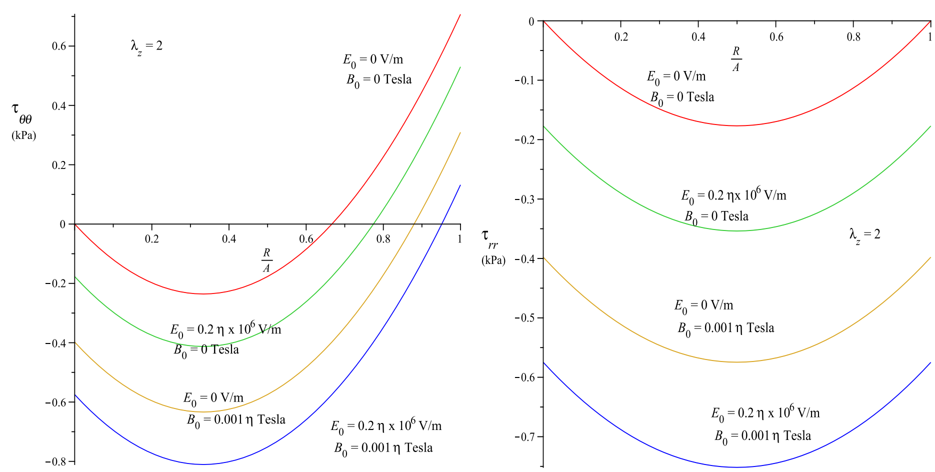

Figure 2: Behaviour of $\tau_{\theta\theta}$ and τ_{rr} at $\lambda_z = 2$ with respect to the changes of E_0 and B_0. The value of $\kappa = 1$ kPa is used for the residual stress

In view of $\boldsymbol{u}_1 = \boldsymbol{E}_R$, $\boldsymbol{u}_2 = \boldsymbol{E}_\theta$ and $\boldsymbol{u}_3 = \boldsymbol{E}_Z$, we obtain $f_1 = f_2 = g_1 = g_2 = 0$, $f_3 = g_3 = 1$, $\zeta_1 = t_1$, $\zeta_2 = t_2$, $\zeta_3 = 0$, $b_L = \dfrac{B_0}{\lambda_z}$ and $e_L = E_0\lambda_z$. The cylindrical components of the Maxwell stress defined in

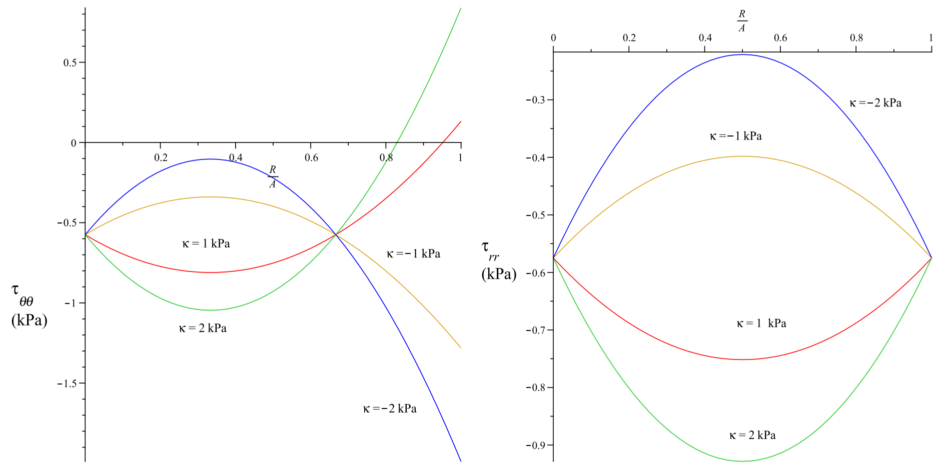

Figure 3: Behaviour of $\tau_{\theta\theta}$ and τ_{rr} at $\lambda_z = 2$, $E_0 = 0.2\eta \times 10^6$ V/m and $B_0 = \eta \times 10^{-3}$ Tesla with respect to the changes in κ

(32) are:

$$(\boldsymbol{T}_M)_{zz} = \frac{B_0^2}{2\mu_0} + \frac{\varepsilon_0 E_0^2}{2} = -(\boldsymbol{T}_M)_{rr} = -(\boldsymbol{T}_M)_{\theta\theta}\,. \tag{73}$$

The non-zero *total stress* components are:

$$\tau_{rr} + p = \lambda_r \frac{\partial \Omega}{\partial \lambda_1}\,, \quad \tau_{\theta\theta} + p = \lambda_r \frac{\partial \Omega}{\partial \lambda_2}\,, \quad \tau_{zz} + p = \lambda_z \frac{\partial \Omega}{\partial \lambda_3}\,. \tag{74}$$

It is evident that the shear stresses are zero and the total stress must satisfy the balance equation

$$r\frac{\mathrm{d}\tau_{rr}}{\mathrm{d}r} = \tau_{\theta\theta} - \tau_{rr}\,, \tag{75}$$

which gives

$$\tau_{rr} = \int_a^r \left(\lambda_r \frac{\partial \Omega}{\partial \lambda_2} - \lambda_r \frac{\partial \tilde{\Omega}}{\partial \lambda_1} \right) \frac{\mathrm{d}r}{r} + (\boldsymbol{T}_M)_{rr}\,, \tag{76}$$

where $a = \dfrac{A}{\sqrt{\lambda_z}}$. We have,

$$\tau_{zz} = \lambda_z \frac{\partial \Omega}{\partial \lambda_3} - \lambda_r \frac{\partial \Omega}{\partial \lambda_1} + \tau_{rr}\,. \tag{77}$$

In view of (76) and (77), τ_{zz} does not depend on the residual stress and takes the form

$$\tau_{zz} = \mu\lambda_z r_1'(\lambda_z) + 0.2\epsilon_0 E_0^2 \lambda_z^3(\lambda_z - 1) + \frac{2B_0^2}{0.01\mu_0}(1 - \frac{1}{\lambda_z}) - \frac{\mu}{\sqrt{\lambda_z}} r_1'(\frac{1}{\sqrt{\lambda_z}}) + \frac{\epsilon_0 E_0^2}{2} + \frac{B_0^2}{2\mu_0}\,. \tag{78}$$

In Fig. 1, the stress-strain curves of τ_{zz} vs λ_z are depicted for various values of E_0 and B_0. If we apply a traction on the "free surface" so that the traction $(\boldsymbol{T}_M)_{rr}$ is eliminated and the surface is free of traction, we would expect the magnitude of τ_{zz} to be larger; this behaviour is indicated in Fig. 1.

The non-axial components are

$$\tau_{rr} = \frac{t_1(R)}{\sqrt{\lambda_z}} - \frac{B_0^2}{2\mu_0} - \frac{\varepsilon_0 E_0^2}{2}\,, \quad \tau_{\theta\theta} = \frac{t_2(R)}{\sqrt{\lambda_z}} - \frac{B_0^2}{2\mu_0} - \frac{\varepsilon_0 E_0^2}{2}\,. \tag{79}$$

Fig. 2 indicates the stresses $\tau_{\theta\theta}$ and τ_{rr} increase as the values of E_0 and B_0 increase. The response of $\tau_{\theta\theta}$ and τ_{rr} to different values of κ is depicted in Fig. 3.

In view of the relations

$$\boldsymbol{h}_L = [\frac{2B_0}{0.01\mu_0\lambda_z}(\lambda_z-1)^2 + \frac{B_0}{\mu_0}\lambda_z]\boldsymbol{E}_Z\,, \quad \boldsymbol{d}_L = [\frac{\varepsilon_0 E_0}{\lambda_z} - 0.2\epsilon_0 E_0\lambda_z(\lambda_z-1)^2]\boldsymbol{E}_Z\,, \tag{80}$$

it is clear that, since λ_z is constant, all the relations in (28) are automatically satisfied.

4.1.3 Extension and Inflation of a Thick-Walled Tube

Here, we examine a non-homogeneous deformation which has several applications. We consider an incompressible thick-walled circular cylindrical tube with initial geometry defined by (66). The resulting deformation for an incompressible solid is described by the equations [46]

$$r^2 - a^2 = \frac{1}{\lambda_z}(R^2 - A^2)\,, \quad \theta = \Theta\,, \quad z = \lambda_z Z\,, \tag{81}$$

where a is the internal radius of the deformed tube and λ_z (constant) is the axial stretch. Note that

$$b^2 - a^2 = \frac{1}{\lambda_z}(B^2 - A^2)\,, \tag{82}$$

where b is the external radius of the deformed tube. The deformation gradient is

$$\boldsymbol{F} = \frac{1}{\lambda\lambda_z}\boldsymbol{e}_r \otimes \boldsymbol{E}_R + \frac{r}{R}\boldsymbol{e}_\theta \otimes \boldsymbol{E}_\Theta + \lambda_z \boldsymbol{e}_z \otimes \boldsymbol{E}_Z\,. \tag{83}$$

Hence, the principal stretches are given by

$$\lambda_1 = \frac{1}{\lambda\lambda_z}\,, \quad \lambda_2 = \lambda = \frac{r}{R}\,, \quad \lambda_3 = \lambda_z\,, \tag{84}$$

where we have introduced the notation λ. The principal directions are

$$\boldsymbol{u}_1 = \boldsymbol{E}_R\,, \quad \boldsymbol{u}_2 = \boldsymbol{E}_\Theta\,, \quad \boldsymbol{u}_3 = \boldsymbol{E}_Z \tag{85}$$

and, $\zeta_1 = t_1$, $\zeta_2 = t_2$ and $\zeta_3 = 0$. Consider the case

$$\boldsymbol{e}_L = E_0\boldsymbol{E}_Z\,, \quad \boldsymbol{b}_L = B_0\boldsymbol{E}_Z\,. \tag{86}$$

We then have $e_L = E_0$, $b_L = B_0$, $f_1 = f_2 = g_1 = g_2 = 0$ and $f_3 = g_3 = 1$. It can be easily shown that $\dfrac{\partial \Omega}{\partial \boldsymbol{e}_L}$ and $\dfrac{\partial \Omega}{\partial \boldsymbol{b}_L}$ depends only on the constant value λ_z, hence the all the conditions in (28) are automatically satisfied.

The non-zero Maxwell stress components are:

$$(\boldsymbol{T}_M)_{zz} = \frac{\varepsilon_0 E_0^2}{2\lambda_z^2} + \frac{\lambda_z^2 B_0^2}{2\mu_0} = -(\boldsymbol{T}_M)_{rr} = -(\boldsymbol{T}_M)_{\theta\theta} \,. \tag{87}$$

The non-zero invariants for this problem are λ, λ_z, $\zeta_1 = t_1$ and $\zeta_2 = t_2$, hence we can write

$$\Omega = W_{(t)}(\lambda, \lambda_z, t_1, t_2) \,. \tag{88}$$

All the shear stresses are zero and this implies that the total stress $\boldsymbol{T}_T$ is coaxial with the left stretch tensor $\boldsymbol{V}$. The principal stresses σ_{rr}, $\sigma_{\theta\theta}$ and σ_{zz} have the following relations

$$\sigma_{\theta\theta} - \sigma_{rr} = \lambda \frac{\partial W_{(t)}}{\partial \lambda} \,, \quad \sigma_{zz} - \sigma_{rr} = \lambda_z \frac{\partial W_{(t)}}{\partial \lambda_z} \,. \tag{89}$$

The equation of equilibrium with negligible body forces reduces to

$$\frac{d\sigma_{rr}}{dr} + \frac{1}{r}(\sigma_{rr} - \sigma_{\theta\theta}) = 0 \,. \tag{90}$$

The above equation is to be solved in conjunction with the boundary conditions

$$\sigma_{rr} = \begin{cases} -P + (\boldsymbol{T}_M)_{rr} & \text{on} \quad r = a \\ (\boldsymbol{T}_M)_{rr} & \text{on} \quad r = b \end{cases} \tag{91}$$

corresponding to an applied pressure P on the inside of the tube. Using (90) and $(89)_1$, we obtain

$$\sigma_{rr} = (\boldsymbol{T}_M)_{rr} - \int_r^b \lambda \frac{\partial W_{(t)}}{\partial \lambda} \, \frac{dr}{r} \,. \tag{92}$$

It follows that

$$P = \int_a^b \lambda \frac{\partial W_{(t)}}{\partial \lambda} \, \frac{dr}{r} \,. \tag{93}$$

For given A and B, noting that from (82), b depends on a and λ_z, Eq. (93) yields an expression for the P that is required to achieve the deformed internal radius a for any given λ_z.

The axial load N needed to hold λ_z fixed can be obtained by the relation

$$\begin{aligned} N &= 2\pi \int_a^b \sigma_{zz} r \, dr = \pi \int_a^b (2\sigma_{zz} - \sigma_{rr} - \sigma_{\theta\theta}) r \, \mathrm{d}r + \pi(b^2 - a^2)\,(\boldsymbol{T}_M)_{rr} + \pi a^2 P \\ &= \pi \int_a^b (2\lambda_z \frac{\partial W_{(t)}}{\partial \lambda_z} - \lambda \frac{\partial W_{(t)}}{\partial \lambda}) r \, dr + \pi(b^2 - a^2)\,(\boldsymbol{T}_M)_{rr} + \pi a^2 P \,. \end{aligned} \tag{94}$$

4.1.4 Simple Torsion of a solid Cylindrical Tube

A cylindrical tube defined by (66) with $A = 0$ is twisted by (the amount of torsional twist per unit deformed length) τ described by the deformation

$$r = R, \quad \theta = \Theta + \tau Z, \quad z = Z, \tag{95}$$

Hence, we have,

$$\boldsymbol{F} \equiv \begin{pmatrix} 1 & 0 & 0 \\ 0 & 1 & \gamma \\ 0 & 0 & 1 \end{pmatrix} , \tag{96}$$

where $\gamma = r\tau$ and

$$\boldsymbol{u}_1 \equiv [1, 0, 0]^T , \quad \boldsymbol{u}_2 \equiv [0, c, s]^T , \quad \boldsymbol{u}_3 \equiv [0, -s, c]^T , \tag{97}$$

where $c^2 + s^2 = 1$. In view of

$$\boldsymbol{F}^T \boldsymbol{F} = \sum_{i=1}^{3} \lambda_i^2 \boldsymbol{u}_i \otimes \boldsymbol{u}_i , \tag{98}$$

we obtain

$$c = \frac{1}{\sqrt{1+\lambda_2^2}} , \quad s = \frac{\lambda_2}{\sqrt{1+\lambda_2^2}} , \tag{99}$$

and

$$\lambda_1 = 1 , \quad \lambda_2 = \frac{s}{c} = \frac{\gamma + \sqrt{\gamma^2 + 4}}{2} \geq 1 , \quad \lambda_3 = \frac{c}{s} = \frac{1}{\lambda_2} \leq 1 . \tag{100}$$

Eqn. (97) implies

$$\zeta_1 = t_1 , \quad \zeta_2 = t_2 c^2 , \quad \zeta_3 = t_2 s^2 . \tag{101}$$

The total stress components:

$$\begin{aligned} &\sigma_{rr} + p = 2l_1 , \quad \sigma_{\theta\theta} + p = 2\left[l_2(s^2(1+\gamma^2) + \gamma cs) + l_3(c^2(1+\gamma^2) - \gamma cs) - 2l_6 cs \right] , \\ &\sigma_{zz} + p = 2\left(l_2 s^2 + l_3 c^2 + 2l_6 cs \right) , \quad \sigma_{z\theta} = 2(l_2\lambda_2^2 - l_3\lambda_3^2)cs + 2l_6\gamma cs , \\ &\sigma_{r\theta} = 2\left[l_4(c + \gamma s) - l_5(s - \gamma c) \right] , \quad \sigma_{zr} = 2\left(l_4 s + l_5 c \right) , \end{aligned} \tag{102}$$

where

$$\begin{aligned} &l_1 = \frac{1}{2\lambda_1}\frac{\partial\Omega}{\partial\lambda_1} , \quad l_2 = \frac{1}{2\lambda_2}\frac{\partial\Omega}{\partial\lambda_2} , \quad l_3 = \frac{1}{2\lambda_3}\frac{\partial\Omega}{\partial\lambda_3} , \\ &l_4 = \left(\frac{\partial\Omega}{\partial\boldsymbol{C}}\right)_{12} , \quad l_5 = \left(\frac{\partial\Omega}{\partial\boldsymbol{C}}\right)_{13} , \quad l_6 = \left(\frac{\partial\Omega}{\partial\boldsymbol{C}}\right)_{23} . \end{aligned} \tag{103}$$

The traction N applied at the ends of the cylinder is

$$N = 2\pi \int_0^A \sigma_{zz} R \, \mathrm{d}R = \pi \int_0^a (2\sigma_{zz} - \sigma_{rr} - \sigma_{\theta\theta}) r \, \mathrm{d}r + \pi a^2 \sigma_{rr}(a) , \quad a = A \tag{104}$$

and the end-cylinder torque

$$M = 2\pi \int_0^A \sigma_{z\theta} R^2 \, \mathrm{d}R \, . \tag{105}$$

Next, we consider two cases for the electromagnetic fields:

Case **A**: $\boldsymbol{b} = B_0 \boldsymbol{e}_r$ and $\boldsymbol{e} = E_0 \boldsymbol{e}_r$.

In this case, we have,

$$f_1 = g_1 = 1 \, , \quad f_2 = f_3 = g_2 = g_3 = 0 \, , \quad b_L = B_0 \, , \quad e_L = E_0 \tag{106}$$

$$\begin{aligned} l_1 &= \frac{1}{2}[t_1 + \varepsilon_0 E_0^2 + \frac{B_0^2}{\mu_0}] \, , \quad l_2 = \frac{1}{2\lambda_2}[\mu r_1'(\lambda_2) + c^2 t_2] \, , \\ l_3 &= \frac{1}{2\lambda_3}[\mu r_1'(\lambda_3) + s^2 t_2] \, , \end{aligned} \tag{107}$$

$$l_4 = 0 \, , \quad l_5 = 0 \, , \quad l_6 = \left(\frac{\partial \Omega}{\partial \boldsymbol{C}} \right)_{23} = -c^2 s^2 t_2 \, . \tag{108}$$

We note that $l_4 = l_5 = 0$ implies $\sigma_{rz} = \sigma_{r\theta} = 0$.

The Maxwell stress components are:

$$(\boldsymbol{T}_M)_{rr} = \frac{B_0^2}{2\mu_0} + \frac{\varepsilon_0 E_0^2}{2} = -(\boldsymbol{T}_M)_{zz} = -(\boldsymbol{T}_M)_{\theta\theta} \, . \tag{109}$$

From the results

$$\boldsymbol{h}_L = \frac{B_0}{\mu_0} \boldsymbol{E}_R \, , \quad \boldsymbol{d}_L = \varepsilon_0 E_0 \boldsymbol{E}_R \, , \tag{110}$$

it is clear that the relations (28) are satisfied, automatically. Using (109), the traction

$$N = \pi \int_0^A (2\sigma_{zz} - t_1(R) - \sigma_{\theta\theta}) R \, \mathrm{d}R \tag{111}$$

and the shear stress

$$\sigma_{z\theta} = \mu[\lambda_2 r'(\lambda_2) - \lambda_3 r'(\lambda_3)] cs - 2\gamma c^3 s^3 t_2(R) \tag{112}$$

indicate that they are independent of the electromagnetic fields B_0 and E_0.

Case **B**: $\boldsymbol{b}_L = B_0 \boldsymbol{E}_R$ and $\boldsymbol{e}_L = E_0 \boldsymbol{E}_z$.

In this case, we have, $\mathrm{Div}\, \boldsymbol{b}_L = 0$, $\mathrm{Curl}\, \boldsymbol{e}_L = \boldsymbol{0}$,

$$f_1 = 1 \, , \quad f_2 = f_3 = 0 \, , \quad g_1 = 0 \, , \quad g_2 = s \, , \quad g_3 = c \, , \quad b_L = B_0 \, , \quad e_L = E_0 \tag{113}$$

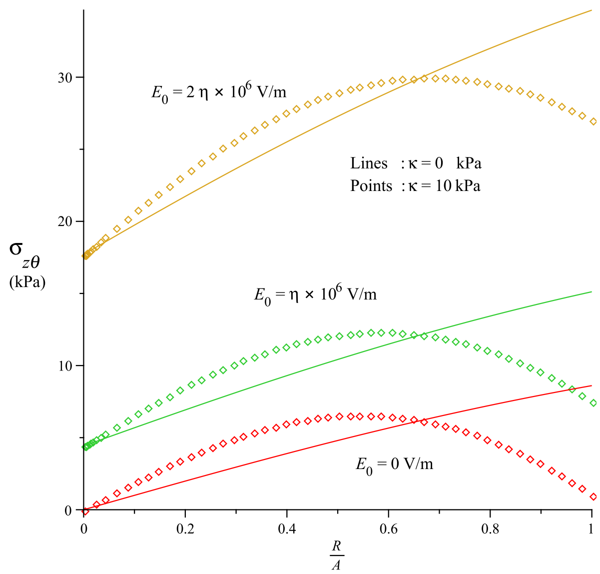

Figure 4: Behaviour of $\sigma_{z\theta}$ at fixed $A\tau = 1$ for various values of E_0 and κ.

and the values of ζ_i are given in (101). The non-zero components of the Maxwell stress are:

$$(\boldsymbol{T}_M)_{rr} = \frac{B_0^2}{2\mu_0} - \frac{\varepsilon_0 E_0^2}{2} = -(\boldsymbol{T}_M)_{zz}\,, \quad (\boldsymbol{T}_M)_{\theta\theta} = -\frac{B_0^2}{2\mu_0} - \frac{\varepsilon_0 E_0^2}{2}\,. \tag{114}$$

It is clear that $l_4 = l_5 = 0$ and this implies that $\sigma_{rz} = \sigma_{r\theta} = 0$ and

$$2l_1 = \zeta_1 + \frac{B_0^2}{\mu_0}\,, \quad l_6 = \frac{\varepsilon_0 E_0^2}{\lambda_2^2 - \lambda_3^2}\left[0.1(r_3(\lambda_2) - r_3(\lambda_3)) - (\frac{1}{2\lambda_2^2} - \frac{1}{2\lambda_3^2})\right] g_2 g_3 - c^2 s^2 t_2\,. \tag{115}$$

The shear stress

$$\sigma_{z\theta} = 2\left(\lambda_2^2 l_2 - \lambda_3^3 l_3\right) cs - 2\gamma c^3 s^3 t_2\,, \tag{116}$$

where

$$2\lambda_\alpha l_\alpha = \mu r_1'(\lambda_\alpha) + \zeta_\alpha r_2'(\lambda_\alpha) + \gamma_\alpha (c_0 E_0^2 r_3'(\lambda_\alpha) + \frac{\varepsilon_0 E_0^2}{\lambda_\alpha^3})\,, \quad \alpha = 2, 3\,. \tag{117}$$

We note that

$$\boldsymbol{d}_L = -\frac{\partial \Omega}{\partial \boldsymbol{e}_L} = -\varepsilon_0 E_0 (\boldsymbol{D}_1 + \boldsymbol{D}_2)\,, \tag{118}$$

where

$$\boldsymbol{D}_1 = [\sum_{i=2}^{3} (0.2 r_3(\lambda_i) - \frac{1}{\lambda_i^2})\gamma_i] \boldsymbol{E}_Z\,, \tag{119}$$

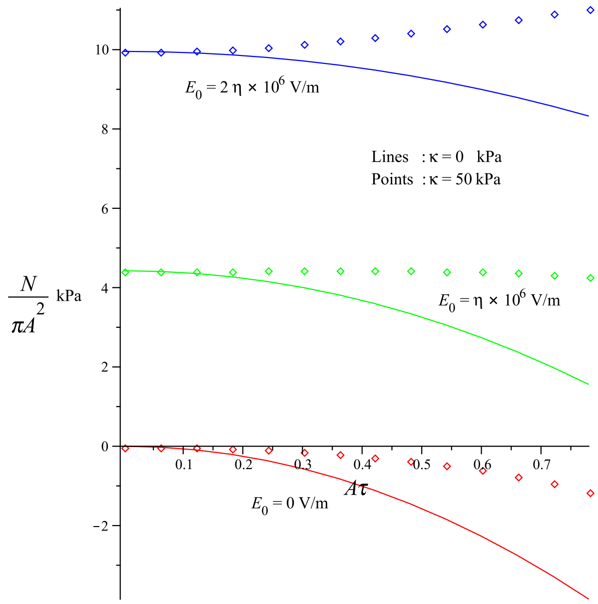

Figure 5: Axial force per unit area $\dfrac{N}{\pi A^2}$ vs $A\tau$ for various values of E_0 and κ.

$$\boldsymbol{D}_2 = (\boldsymbol{I} - \boldsymbol{E}_Z \otimes \boldsymbol{E}_Z) \sum_{i=2}^{3} [0.2 r_3(\lambda_i) - \frac{1}{\lambda_i^2}] g_i \boldsymbol{u}_i \tag{120}$$

and

$$\boldsymbol{h}_L = \frac{\partial \Omega}{\partial \boldsymbol{b}_L} = \frac{B_0}{\mu_0} \boldsymbol{E}_R \,. \tag{121}$$

In view of (118) and (121), we have the required condition $\operatorname{Div} \boldsymbol{d}_L = 0$ and $\operatorname{Curl} \boldsymbol{h}_L = \mathbf{0}$.

The applied traction

$$N = \pi \int_0^A (2\sigma_{zz} - t_1(R) - \sigma_{\theta\theta}) R \, \mathrm{d}R - \pi A^2 \frac{\varepsilon_0 E_0^2}{2} \tag{122}$$

and the shear stress $\sigma_{z\theta}$ are both independent of the magnetic field B_0 . The effects of residual stress and magneto-electric fields, for Case **B**, on the shear stress $\sigma_{z\theta}$ field are depicted in Fig. 4. We also illustrate the dependence of the normal traction per-unit area $\dfrac{N}{\pi A^2}$ on τ in Fig. 5 for a couple values of E_0 and κ.

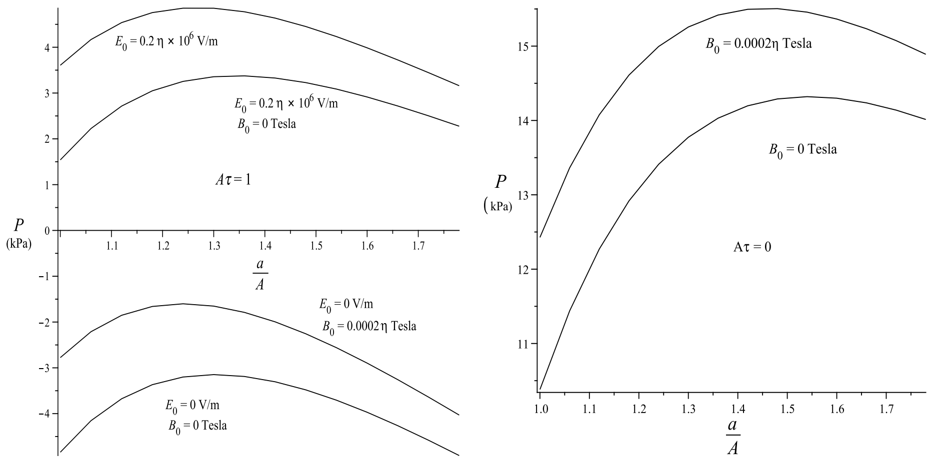

Figure 6: P vs $\dfrac{a}{A}$ at $\lambda_z = 2$ for various values of E_0 and B_0. The value of $\kappa = 1$ kPa is used for the residual stress.

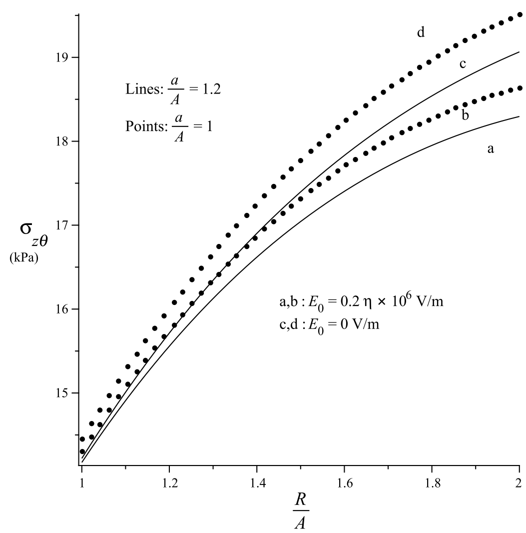

Figure 7: Behaviour of $\sigma_{z\theta}$ at $A\tau = 1$, $\lambda_z = 2$ and $\kappa = 1$ (kPa) for various values of E_0.

4.1.5 Extension, inflation and torsion of a cylinder tube

In this section we consider an incompressible thick-walled circular cylindrical tube with the initial geometry defined by (66). The deformation is described by [46]

$$r^2 = a^2 + \frac{R^2 - A^2}{\lambda_z}, \quad \theta = \Theta + \lambda_z \tau Z, \quad z = \lambda_z Z, \tag{123}$$

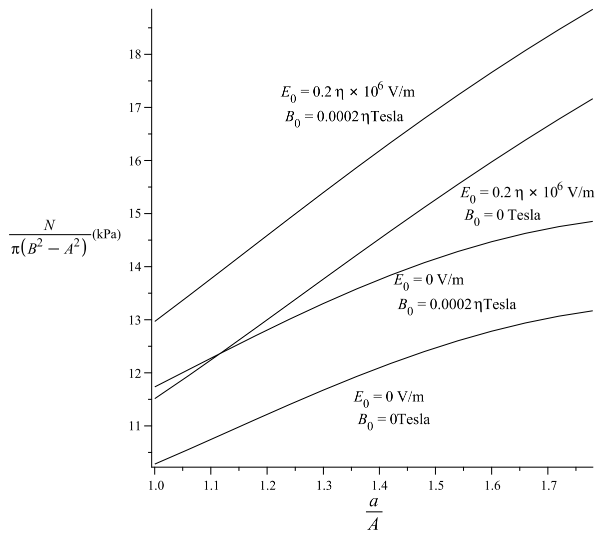

Figure 8: $\dfrac{N}{\pi(B^2 - A^2)}$ vs $\dfrac{a}{A}$ at $A\tau = 1$, $\lambda_z = 2$ and $\kappa = 1$ (kPa) for various values of E_0 and B_0.

where τ is the amount of torsional twist per unit deformed length and λ_z is the axial stretch. The deformation gradient

$$\boldsymbol{F} = \lambda_r \boldsymbol{e}_r \otimes \boldsymbol{E}_R + \lambda_\theta \boldsymbol{e}_\theta \otimes \boldsymbol{E}_\Theta + \gamma \lambda_z \boldsymbol{e}_\theta \otimes \boldsymbol{E}_Z + \lambda_z \boldsymbol{e}_Z \otimes \boldsymbol{E}_Z \,, \tag{124}$$

where

$$\gamma = r\tau \,, \quad \lambda_\theta = \frac{r}{R} \,, \quad \lambda_r = \frac{1}{\lambda_\theta \lambda_z} \,. \tag{125}$$

The Lagrangian principal directions have cylindrical components:

$$\boldsymbol{u}_1 \equiv [1, 0, 0]^T \,, \quad \boldsymbol{u}_2 \equiv [0, c, s]^T \,, \quad \boldsymbol{u}_3 \equiv [0, -s, c]^T \,, \tag{126}$$

where $c^2 + s^2 = 1$. Using (98) and (126), we obtain

$$c = \cos(\phi) = \frac{2}{\sqrt{2(\hat{\gamma}^2 + 4) + 2\hat{\gamma}\sqrt{\hat{\gamma}^2 + 4}}}, \quad s = \sin(\phi) = \frac{\hat{\gamma} + \sqrt{\hat{\gamma}^2 + 4}}{\sqrt{2(\hat{\gamma}^2 + 4) + 2\hat{\gamma}\sqrt{\hat{\gamma}^2 + 4}}} \,, \tag{127}$$

where

$$\hat{\gamma} = \frac{\lambda_z^2(\gamma^2 + 1) - \lambda_\theta^2}{\gamma \lambda_\theta \lambda_z} \,. \tag{128}$$

Using the relation

$$c^2 - s^2 = -\hat{\gamma} c s \,, \tag{129}$$

we derive the relation

$$\tan 2\phi = -\frac{2}{\hat{\gamma}}\,. \tag{130}$$

In view of (130) and the possibility that $\hat{\gamma}$ may have a zero value, we have the constraint

$$0 \le \phi \le \frac{\pi}{2} \tag{131}$$

The principal stretches are

$$\lambda_1 = \lambda_r\,, \quad \lambda_2 = \sqrt{\lambda_\theta^2 + \frac{\lambda_\theta\lambda_z\gamma s}{c}}\,, \quad \lambda_3 = \sqrt{\lambda_\theta^2 - \frac{\lambda_\theta\lambda_z\gamma c}{s}} \tag{132}$$

and the residual stress invariants ζ_i are given by (101).

In this section, we only consider the case for $\boldsymbol{e}_L = E_0\boldsymbol{E}_Z$ and $\boldsymbol{b}_L = B_0\boldsymbol{E}_R$ and, we have,

$$b_L = B_0\,, \quad e_L = E_0\,, \quad \boldsymbol{f} = \boldsymbol{E}_R\,, \quad \boldsymbol{g} = \boldsymbol{E}_Z\,, \quad f_1 = 1\,, \quad f_2 = f_3 = 0\,, \quad g_1 = 0\,, \quad g_2 = s\,, \quad g_3 = c\,. \tag{133}$$

The cylindrical components of the total stress take the form:

$$\begin{aligned}
&\sigma_{rr} = 2\lambda_r^2 l_1 - p\,,\\
&\sigma_{\theta\theta} = 2\left[l_2(c^2\lambda_\theta^2 + s^2\gamma^2\lambda_z^2) + l_3(s^2\lambda_\theta^2 + c^2\gamma^2\lambda_z^2) + \gamma\lambda_\theta\lambda_z[(l_2 - l_3)cs + l_6(c^2 - s^2)]\right.\\
&\qquad \left. + 2l_6cs(\gamma^2\lambda_z^2 - \lambda_\theta^2)\right] - p\,,\\
&\sigma_{zz} = 2\lambda_z^2(l_2s^2 + l_3c^2 + 2l_6cs) - p\,,\\
&\sigma_{r\theta} = 2\lambda_r\left[\lambda_\theta(l_4c - l_5s) + \gamma\lambda_z(l_4s + l_5c)\right]\,, \qquad \sigma_{rz} = 2\lambda_r\lambda_z(l_4s + l_5c)\\
&\sigma_{z\theta} = 2\left[\lambda_\theta\lambda_z[(l_2 - l_3)cs + l_6(c^2 - s^2)] + \gamma\lambda_z^2(l_2s^2 + l_3c^2 + 2l_6cs)\right]\,,
\end{aligned} \tag{134}$$

where $l_1, l_2, \ldots, l_6$ are given by (103). In view of (101) and (133), we have $l_4 = l_5 = 0$,

$$\begin{aligned}
&l_1 = \frac{1}{2\lambda_1}\left[\mu r_1'(\lambda_1) + \zeta_1 r_2'(\lambda_1) + c_1(b_L)r_4'(\lambda_1) + \frac{B_0^2}{\mu_0}\lambda_1\right]\\
&l_\alpha = \frac{1}{2\lambda_\alpha}\left[\mu r_1'(\lambda_\alpha) + \zeta_\alpha r_2'(\lambda_\alpha) + c_0(e_L)\gamma_\alpha r_3'(\lambda_2) + \varepsilon_0 e_L^2\frac{\gamma_\alpha}{\lambda_\alpha^3}\right]\,, \quad \alpha = 2, 3\,,\\
&l_6 = \frac{cs}{\lambda_2^2 - \lambda_3^2}\left(\gamma_{(2)} - \gamma_{(3)}\right) - c^2s^2t_2\,, \quad \gamma_{(\alpha)} = c_0(e_L)r_3(\lambda_\alpha) - \frac{\varepsilon_0 e_L^2}{2\lambda_\alpha^2}\,, \quad \alpha = 2, 3\,.
\end{aligned} \tag{135}$$

It is clear that $\sigma_{rz} = \sigma_{r\theta} = 0$ and all the conditions in (28) are automatically satisfied.

The Maxwell stress components are:

$$(\boldsymbol{T}_M)_{rr}(r) = -\frac{\varepsilon_0 E_0^2}{2\lambda_z^2} + \frac{\lambda_r^2 B_0^2}{2\mu_0}\,, \quad (\boldsymbol{T}_M)_{\theta\theta}(r) = -\frac{\varepsilon_0 E_0^2}{2\lambda_z^2} - \frac{\lambda_r^2 B_0^2}{2\mu_0}\,, \tag{136}$$

$$(\boldsymbol{T}_M)_{zz}(r) = \frac{\varepsilon_0 E_0^2}{2\lambda_z^2} - \frac{\lambda_r^2 B_0^2}{2\mu_0}\,, \tag{137}$$

taking note that the Maxwell stress is not constant but depends on r.

If we solve the equilibrium equation (90) with the boundary tractions

$$\sigma_{rr} = \begin{cases} -P + (\boldsymbol{T}_M)_{rr}(a) & \text{on} \quad r = a \\ (\boldsymbol{T}_M)_{rr}(b) & \text{on} \quad r = b \end{cases} \tag{138}$$

where P is the applied pressure on the inside of the tube, we obtain

$$P = \int_a^b \frac{\sigma_{\theta\theta} - \sigma_{rr}}{r}\, dr + (\boldsymbol{T}_M)_{rr}(a) - (\boldsymbol{T}_M)_{rr}(b)\,. \tag{139}$$

The total traction N applied at the ends of the cylinder are as follows:

$$N = 2\pi \int_a^b \sigma_{zz} r\,\mathrm{d}r = \pi \int_a^b (2\sigma_{zz} - \sigma_{rr} - \sigma_{\theta\theta}) r\,\mathrm{d}r + \pi(b^2\,(\boldsymbol{T}_M)_{rr}(b) - a^2[(\boldsymbol{T}_M)_{rr}(a) - P]) \tag{140}$$

For plotting purposes, without loss of generality, we use $A = 1$ and $B = 2A$. The internal pressure P vs $\dfrac{a}{A}$ is depicted in Fig. 6. When $A\tau = 0$, it can be easily shown that P is independent of B_0. In Fig. 6_2 the curves for $A\tau = 0$ are depicted; these curves represent the deformation of an extension and inflation of a thick-walled tube described in Section 4.1.3 for $\boldsymbol{e}_L = E_0\boldsymbol{E}_Z$ and $\boldsymbol{b}_L = B_0\boldsymbol{E}_R$.

It is clear from (134) and (135) that the shear stress $\sigma_{z\theta}$ is independent of B_0 and this is potrayed in Fig. 7 for some values of $\dfrac{a}{A}$ and E_0. The dependence of $\dfrac{N}{\pi(B^2 - A^2)}$ on $\dfrac{a}{A}$ at $A\tau = 1$, $\lambda_z = 2$ and $\kappa = 1$ (kPa) for various values of E_0 and B_0 is illustrated in Fig. 8.

4.2 Residual stress on a thin rectangular sheet

Consider an undeformed configuration of a thin rectangular sheet described by

$$-A \le X \le A\,, \quad -B \le Y \le B\,, -L \le Z \le L\,, \tag{141}$$

where (X, Y, Z) is a Cartesian reference configuration point corresponding to the Cartesian basis $\{\boldsymbol{g}_1, \boldsymbol{g}_2, \boldsymbol{g}_3\}$ and $L << 1$. In order to study the effect of residual stress on a thin rectangular sheet discussed in Section 4.2.1 below, we require a specific residual stress field to illustrate our results, and in view of this, we consider the specific residual stress field

$$\boldsymbol{T}_R = s_{11}\boldsymbol{g}_1 \otimes \boldsymbol{g}_1 + s_{22}\boldsymbol{g}_2 \otimes \boldsymbol{g}_2 + s_{12}(\boldsymbol{g}_1 \otimes \boldsymbol{g}_2 + \boldsymbol{g}_2 \otimes \boldsymbol{g}_1)\,, \tag{142}$$

where

$$\begin{aligned} s_{11} &= 4\kappa(1 - \frac{X^2}{A^2})^2(\frac{3Y^2}{B^2} - 1)\,, \quad s_{22} = 4\kappa\frac{B^2}{A^2}(1 - \frac{Y^2}{B^2})^2(\frac{3X^2}{A^2} - 1)\,, \\ s_{12} &= 16\kappa\frac{XY}{A^2}(1 - \frac{X^2}{A^2})(\frac{Y^2}{B^2} - 1)\,, \end{aligned} \tag{143}$$

where κ has the dimension of stress. It is clear that the residual stress field (143) satisfies the equilibrium equation and stress free condition in the reference configuration.

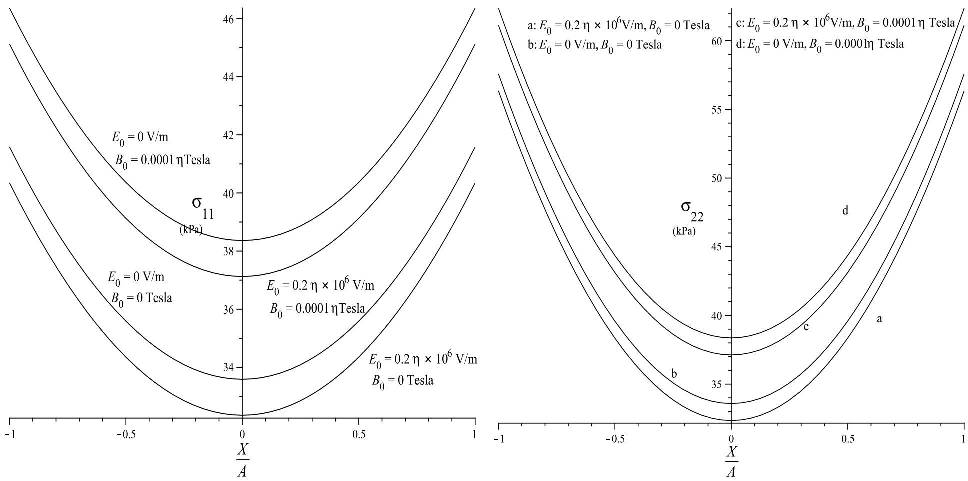

Figure 9: Stresses σ_{11} and σ_{22} along the X-axis at $Y = 0$ when $\lambda = 2$ and $\kappa = 1$ for various values of E_0 and B_0.

4.2.1 Equibiaxial tension

It is noted that if we simply stretch a residually stressed rectangular slab material, the deformation may not be homogeneous due to the presence of residual stresses. However, in this paper, for simplicity, we assume a homogenous stretch defined in (144) below and require a non-homogeneous stress to maintain the homogeneous deformation described by

$$\boldsymbol{F} = \lambda \boldsymbol{g}_1 \otimes \boldsymbol{g}_1 + \lambda \boldsymbol{g}_2 \otimes \boldsymbol{g}_2 + \frac{1}{\lambda^2} \boldsymbol{g}_3 \otimes \boldsymbol{g}_3. \tag{144}$$

Note that all vector and tensor components are relative to the basis $\{\boldsymbol{g}_1, \boldsymbol{g}_2, \boldsymbol{g}_3\}$. In this case, we have, $\boldsymbol{u}_i = \boldsymbol{g}_i$ and we only study the case $\boldsymbol{e} = E_0 \boldsymbol{g}_3$ and $\boldsymbol{b} = B_0 \boldsymbol{g}_3$. Hence,

$$\lambda_1 = \lambda_2 = \lambda\,, \quad \lambda_3 = \frac{1}{\lambda^2}\,, \quad f_1 = f_2 = g_1 = g_2 = 0\,, \quad f_3 = g_3 = 1 \tag{145}$$

and $\boldsymbol{b}_L = B_0 \lambda^2 \boldsymbol{g}_3$ and $\boldsymbol{e}_L = \dfrac{E_0}{\lambda^2} \boldsymbol{g}_3$. The Maxwell stress components take the form

$$(\boldsymbol{T}_M)_{33} = \frac{B_0^2}{2\mu_0} + \frac{\varepsilon_0 E_0^2}{2} = -(\boldsymbol{T}_M)_{11} = -(\boldsymbol{T}_M)_{22}\,. \tag{146}$$

We express the total stress in the form

$$\boldsymbol{T}_T = 2\boldsymbol{F} \frac{\partial W_m}{\partial \boldsymbol{C}} \boldsymbol{F}^T + 2\boldsymbol{F} \frac{\partial I_T}{\partial \boldsymbol{C}} \boldsymbol{F}^T - p\boldsymbol{I}\,, \tag{147}$$

where

$$W_m = \mu \sum_{i=1}^{3} r_1(\lambda_i) + N_1 + N_2 + \frac{b_L^2}{2\mu_0} \sum_{i=1}^{3} \beta_i \lambda_i^2 - \frac{\epsilon_0 e_L^2}{2} \sum_{i=1}^{3} \frac{\gamma_i}{\lambda_i^2}\,, \tag{148}$$

and, in view of $r_2(x) = x - 1$,

$$I_T = \operatorname{tr}(\boldsymbol{T}_R(\boldsymbol{U} - I)) = \sum_{i=1}^{3} \zeta_i(\lambda_i - 1)\,. \tag{149}$$

For equibiaxial deformations and for the residual stress given in Section 4.2, we have,

$$\operatorname{div} 2\boldsymbol{F}\frac{\partial I_T}{\partial \boldsymbol{C}}\boldsymbol{F}^T = \operatorname{Div}\boldsymbol{T}_R = 0\,. \tag{150}$$

Let σ_{ij} be the spectral components of $\boldsymbol{T}_T$, since,

$$\sigma_{33} = (\boldsymbol{T}_M)_{33}. \tag{151}$$

It is clear that, in view of (150) and (151)

$$p = \lambda_3\left[\mu r_1'(\lambda_3) + c_0(e_L)r_3'(\lambda_3) + c_1(b_L)r_4'(\lambda_3) + \frac{b_L^2\lambda_3}{\mu_0} + \frac{\varepsilon_0 e_L^2}{\lambda_3^3}\right] - \frac{B_0^2}{2\mu_0} - \frac{\varepsilon_0 E_0^2}{2} \tag{152}$$

and

$$\operatorname{div} \boldsymbol{T}_T = 0 \tag{153}$$

is automatically satisfied. Furthermore, all the relations in (28) are also automatically satisfied. The non-zero stress components are

$$\sigma_{11} = \mu\lambda r_1'(\lambda) + \lambda s_{11} - p\,, \tag{154}$$

$$\sigma_{22} = \mu\lambda r_1'(\lambda) + \lambda s_{22} - p\,, \quad \sigma_{12} = \lambda s_{12}\,. \tag{155}$$

The influence of residual stress and electro-magnetic fields on σ_{11} and σ_{22} stress fields are depicted in Fig. 9. The figures are depicted using $A = B = 1$.

5 Conclusion

In this paper, a spectral invariant-based model for nonlinear magneto-electro-elastic materials in the presence of residual stresses is presented. The proposed potential function contains single variable functions that depend on a spectral invariant with a clear physical meaning; this facilitates the creation of specific forms of the total energy function, in the sense that a single variable function with a clear physical argument can be easily handled and is experimentally attractive. The advantages of spectral invariants over classical invariants [67] are discussed in reference [65]. After omitting the invariants e_L and b_L, we have shown that only 13 spectral invariants are independent, which is far less than the 37 classical invariants in the corresponding minimal integrity basis [67]; hence this may aid in reducing the complexity of modelling nonlinear residually stressed magneto-electro-elastic solids. Analyses of several inhomogeneous boundary value problems are given in which these results can be used to validate experimental data. It is clearly indicated in Section 4 that residual stress and electromagnetic fields significantly influence the mechanical behaviour of elastic solid deformations. The model developed here is novel. The time-independent framework, developed here, will be extended to incorporate time-dependent phenomena in a forthcoming contribution.

Appendix A

In view of $(1)_{3,5}$, we have

$$\operatorname{div}(\boldsymbol{d}\otimes\boldsymbol{e}) = (\operatorname{grad}\boldsymbol{e})\boldsymbol{d} = \varepsilon_0(\operatorname{grad}\boldsymbol{e})\boldsymbol{e} + (\operatorname{grad}\boldsymbol{e})\boldsymbol{p}\,, \quad \operatorname{div}\frac{(\boldsymbol{e}\cdot\boldsymbol{e})\boldsymbol{I}}{2} = (\operatorname{grad}\boldsymbol{e})^T\boldsymbol{d}\,. \tag{A1}$$

Using the relations

$$[(\operatorname{grad}\boldsymbol{e}) - (\operatorname{grad}\boldsymbol{e})^T]\boldsymbol{e} = \operatorname{curl}\boldsymbol{e}\times\boldsymbol{e}\,, \quad [(\operatorname{grad}\boldsymbol{e}) - (\operatorname{grad}\boldsymbol{e})^T]\boldsymbol{p} = \operatorname{curl}\boldsymbol{e}\times\boldsymbol{p}\,, \tag{A2}$$

we have

$$\operatorname{div}[\boldsymbol{d}\otimes\boldsymbol{e} - \frac{1}{2}\varepsilon_0(\boldsymbol{e}\cdot\boldsymbol{e})\boldsymbol{I}] = (\operatorname{grad}\boldsymbol{e})^T\boldsymbol{p} + curl\boldsymbol{e}\times\boldsymbol{p} + \varepsilon_0\operatorname{curl}\boldsymbol{e}\times\boldsymbol{e}\,. \tag{A3}$$

In view of the relation $\operatorname{curl}\boldsymbol{e} = -\dot{\boldsymbol{b}}$ we obtain,

$$\operatorname{div}[\boldsymbol{d}\otimes\boldsymbol{e} - \frac{1}{2}\varepsilon_0(\boldsymbol{e}\cdot\boldsymbol{e})\boldsymbol{I}] = (\operatorname{grad}\boldsymbol{e})^T\boldsymbol{p} - \dot{\boldsymbol{b}}\times\boldsymbol{p} - \varepsilon_0\dot{\boldsymbol{b}}\times\boldsymbol{e} = (\operatorname{grad}\boldsymbol{e})^T\boldsymbol{p} - \dot{\boldsymbol{b}}\times\boldsymbol{d} \tag{A4}$$

and hence Eqn. (6). Using the relations

$$\operatorname{div}(\boldsymbol{b}\otimes\boldsymbol{b}) = (\operatorname{grad}\boldsymbol{b})\boldsymbol{b}\,, \quad \operatorname{div}\frac{(\boldsymbol{b}\cdot\boldsymbol{b})\boldsymbol{I}}{2} = (\operatorname{grad}\boldsymbol{b})^T\boldsymbol{b}\,, \quad [(\operatorname{grad}\boldsymbol{b}) - (\operatorname{grad}\boldsymbol{b})^T]\boldsymbol{b} = \operatorname{curl}\boldsymbol{b}\times\boldsymbol{b}\,, \tag{A5}$$

we have, in view of $(1)_{4,6}$

$$\frac{1}{\mu_0}\operatorname{div}[\boldsymbol{b}\otimes\boldsymbol{b} - \frac{(\boldsymbol{b}\cdot\boldsymbol{b})\boldsymbol{I}}{2}] = \frac{1}{\mu_0}\operatorname{curl}\boldsymbol{b}\times\boldsymbol{b} = \dot{\boldsymbol{d}}\times\boldsymbol{b} + (\operatorname{curl}\boldsymbol{m})\times\boldsymbol{b}\,. \tag{A6}$$

In view of $(1)_1$, we have the relations

$$\operatorname{div}(\boldsymbol{m}\cdot\boldsymbol{b})\boldsymbol{I} = (\operatorname{grad}\boldsymbol{b})^T\boldsymbol{m} + (\operatorname{grad}\boldsymbol{m})^T\boldsymbol{b}\,, \quad \operatorname{div}(\boldsymbol{b}\otimes\boldsymbol{m}) = (\operatorname{grad}\boldsymbol{m})^T\boldsymbol{b}\,. \tag{A7}$$

Using the relation

$$[(\operatorname{grad}\boldsymbol{m}) - (\operatorname{grad}\boldsymbol{m})^T]\boldsymbol{b} = \operatorname{curl}\boldsymbol{m}\times\boldsymbol{b} \tag{A8}$$

we obtain

$$\operatorname{div}[(\boldsymbol{m}\cdot\boldsymbol{b})\boldsymbol{I} - \boldsymbol{b}\otimes\boldsymbol{m}] = (\operatorname{grad}\boldsymbol{b})^T\boldsymbol{m} - (\operatorname{curl}\boldsymbol{m})\times\boldsymbol{b}\,. \tag{A9}$$

Equation (9) can be obtained from (A9) and (A6).

Acknowledgements:

M. Hossain acknowledges the support of Engineering and Physical Sciences Research Council (EPSRC) under an Impact Acceleration Award (EP/R511614/1) to this work.

References

[1] Ahamed, T. , Dorfmann, L. , Ogden, R. W. (2016). Modelling of residually stressed materials with application to AAA, *Journal of the Mechanical Behavior of Biomedical Materials*, **61**, 221 -234.

[2] Amjadi, M., Pichitpajongkit, A., Lee, S., Ryu, S., Park, I. (2012). Highly stretchable and sensitive strain sensor based on silver nanowire-elastomer nanocomposite, *ACS Nano*, **8**, 5154–5163.

[3] Barthelemy, M. , Bibes, A. (2008). Multiferroics: towards a magnetoelectric memory, *Nature Materials*, **7**, 425–426.

[4] Bastola, A. K. , Hossain, M. (2020). A review on magneto-mechanical characterizations of magnetorheological elastomers, *Composites Part B: Engineering*, **200**, 108348.

[5] Bednarek, S. (1999). The giant magnetostriction in ferromagnetic composites within an elastomer matrix, *Applied Physics A*, **68**, 63–67.

[6] Bellan, C. , Bossis, G. (2002). Field dependence of viscoelastic properties of MR elastomers, *International Journal of Modern Physics B*, **16**, 2447–2453.

[7] Bica, I. (2012). The influence of the magnetic field on the elastic properties of anisotropic magnetorheological elastomers, *Journal of Industrial and Engineering Chemistry*, **18**, 1666 - 1669.

[8] Boczkowska, A. , Awietjan, S. F. (2009). Smart composites of urethane elastomers with carbonyl iron, *Journal of Material Science*, **44**, 4104–4111.

[9] Brigadnov, I.A., Dorfmann, A. (2003). Mathematical modeling of magneto-sensitive elastomers. *International Journal of Solids and Structures*, **40**, 4659 - 4674.

[10] Bustamante, R., Dorfmann, A. Ogden R.W. (2007). On variational formulations in nonlinear magnetoelastostatics.*Mathematics and Mechanics of Solids*, **13 (8)**, 725- - 745.

[11] Bustamante, R., Shariff, M.H.B.M., Hossain, M. (2020). Mathematical formulations for elastic magneto-electrically coupled soft materials at finite strains: Time-independent processes. *International Journal of Engineering Science*, **159**, 103429.

[12] Bustamante, R. (2010). Transversely isotropic nonlinear magneto-active elastomers, *Acta Mechanica*, **210**, 183–214.

[13] Dang, Z. M., Yuan, J. K., Zha, J. W., Zhou, T., Li, S. T. , Hu, G. H. (2012). Fundamentals, processes and applications of high-permittivity polymer-matrix composites, *Progress in Materials Science*, **57**, 660–723.

[14] Du, Y., Lü, C., Destrade, M. , Chen, W. (2019). Influence of initial residual stress on growth and pattern creation for a layered aorta, *Scientific Reports*, **9(1)**, 1–9.

[15] Du, Y., Lü, C., Liu, C., Han, Z., Li, J., Chen, W., Qu, S., , Destrade, M. (2019). Prescribing patterns in growing tubular soft matter by initial residual stress, *Soft matter*, **15(42)**, 8468 - 8474.

[16] Dorfmann, A. , Brigdanov, I. A. (2004). Constitutive modelling of magneto-sensitive Cauchy elastic solids, *Computational Materials Science*, **29**, 270–282.

[17] Dorfmann, A. , Ogden, R. W. (2003). Magnetoelastic modelling of elastomers, *European Journal of Mechanics A/Solids*, **22**, 497–507.

[18] M El Hamdaoui, M., Merodio, J. , Ogden, R.W. (2020). Two-phase piecewise homogeneous plane deformations of a fibre-reinforced neo-Hookean material with application to fibre kinking and splitting. *Journal of the Mechanics and Physics of Solids*, **143**, 104091.

[19] Eerenstein, W., Mathur, N. D. , Scott, J. F. (2006). Multiferroic and magnetoelectric materials. *Nature*, **442**, 759–765.

[20] Eringen, A. C. , Maugin, G. A. (1990). Electrodynamics of Continua , Springer-Verlag.

[21] Fetisov, Y. K., Bush, A. A., Kamentsev, K. E., Ostashchenko, Y. A. , Srinivasan, G. (2006). Ferritepiezoelectric multilayers for magnetic field sensors, *IEEE. Sensors Journal*, **6**, 935 - 938.

[22] Fiebig, M. (2005). Revival of the magnetoelectric effect, *Journal of Physics D: Applied Physics*, **38**, R123.

[23] Garcia-Gonzalez, D. , Hossain, M. (2021). A microstructural-based approach to model magneto-viscoelastic materials at finite strains, *International Journal of Solids and Structure*, **208-209**:119-132

[24] Gich, M., Fina, I., Morelli, F., Sánchez, A., Alexe, J., Gázquez, M., Fontcuberta, J. , Roig, A. (2014). Multiferroic iron oxide thin films at room temperature, *Advanced Materials*, **26**, 4645–4652.

[25] Gower, A.L., Ciarletta, P. , Destrade, M. (2015). Initial stress symmetry and its applications in elasticity, *Proceedings of the Royal Society A: Mathematical, Physical and Engineering Sciences* , **471**(2183):20150448.

[26] Gower, A.L., Shearer, T. , P. Ciarletta. (2017). A new restriction for initially stressed elastic solids, *The Quarterly Journal of Mechanics and Applied Mathematics*, **70(4)**, 455–478.

[27] Hoger, A. (1986). On the determination of residual stress in an elastic body, Journal of Elasticity, **16**:302-324

[28] Hossain, M., Saxena, P. , Steinmann, P. (2015). Modelling the mechanical aspects of the curing process of magneto-sensitive elastomeric materials, *International Journal of Solids and Structures*, **58**, 257–269.

[29] Hossain, M., Chatzigeorgiou, G., Meraghni, F. , Steinmann, P. (2015). A multi-scale approach to model the curing process in magneto-sensitive polymeric materials, *International Journal of Solids and Structures*, **69-70**, 34–44.

[30] Hossain, M., Saxena, P., Steinmann, P. (2015). Modelling the curing process in magneto-sensitive polymers: rate-dependence and shrinkage, International Journal of Non-Linear Mechanics, **74**: 108-121

[31] Hu, W., Lum, G. Z., Mastrangeli, M. , Sitti, M. (2018). Small-scale soft-bodied robot with multimodal locomotion, *Nature*, **554**, 81–85.

[32] Jha, N.K., Reinoso, J., Dehghani, H. , Merodio, J. (2019). Constitutive modeling framework for residually stressed viscoelastic solids at finite strains. *Mechanics Research Communications*, **95**, 79 - 84.

[33] Kim, Y., Yuk, H., Zhao, R., Chester, S. A. , Zhao, X. (2018). Printing ferromagnetic domains for untethered fast-transforming soft materials, *Nature*, **558**, 274–279.

[34] Kovetz, A. (2000). Electromagnetic Theory. University Press, Oxford.

[35] Krichen, S., Liu, L. , Sharma, P. (2017). Biological cell as a soft magnetoelectric material: elucidating the physical mechanisms underpinning the detection of magnetic fields by animals, *Physics Review E*, 96, 042404.

[36] Li, S., Bai, H., Shepherd, R. F., Zhao, H. (2019). Bio-inspired Design and Additive Manufacturing of Soft Materials, Machines, Robots, and Haptic Interfaces, *Angewandte Chemie International Edition*, **58**, 11182-11204

[37] Liu, L. , Sharma, P. (2013). Giant and universal magnetoelectric coupling in soft materials and concomitant ramifications for materials science and biology, *Physics Review E*, **88**, 040601.

[38] Liu, L. (2014). An energy formulation of continuum magneto-electro-elasticity with applications, *Journal of Mechanics and Physics of Solids*, **63**, 451–480.

[39] Maugin, G. A. (1988). Continuum Mechanics of Electromagnetic Solids, North Holland, Amsterdam.

[40] Mehnert, M., Hossain, M. , Steinmann, P. (2016). On nonlinear thermo-electro-elasticity, *Proceedings of the Royal Society A*, **472**, 20160170.

[41] Mehnert, M., Hossain, M., Steinmann, P. (2019). Experimental and numerical investigations of the electro-viscoelastic behavior of VHB 4905, *European Journal of Mechanics-A/Solids*, **77**, 103797

[42] Monk, P. (2003). Finite Element Methods for Maxwell Equations, Oxford University Press, Clarendon.

[43] Merodio, J., Ogden, R. W., , Rodriguez, J. (2013). The influence of residual stress on finite deformation elastic response. *International Journal of Non-linear Mechanics*, **56**:43-49.

[44] Merodio, J. , Ogden, R.W. (2016). Extension, inflation and torsion of a residually stressed circular cylindrical tube, *Continuum Mechanics and Thermodynamics*, **28** (1-2): 157-174.

[45] Nan, C. W., Bichurin, M. I., Dong, S., Viehland, D. , Srinivasan, G. (2008). Multiferroic magnetoelectric composites: historical perspective, status, and future directions, *Journal of Applied Physics*, **103**, 031101.

[46] Ogden, R. W. (1997). Non-linear Elastic Deformations, Dover, New York.

[47] Ogden, R.W. , Singh, B. (2011). Propagation of waves in an incompressible transversely isotropic elastic solid with initial stress: Biot revisited, *Journal of Mechanics of Materials and Structures*, **6(1)**, 453 - 477.

[48] Pao, Y. H. (1978). Electromagnetic forces in deformable continua, *Mechanics Today*, (Nemat- Nasser, S., ed.), Oxford: Pergamon Press. 4, 209–306.

[49] Pyatakov, A. P. , Zvezdin, A. K. (2012). Magnetoelectric and multiferroic media, *Physics-Uspekhi*, **55**, 557.

[50] Rambausek, M. , Keip, M. A. (2018). Analytical estimation of non-local deformation-mediated magneto-electric coupling in soft composites, *Proceedings of the Royal Society A*, **474**, 20170803.

[51] Shams, M., Destrade, M. , Ogden, R.W. (2011). Initial stresses in elastic solids: Constitutive laws and acoustoelasticity. *Wave Motion* **48**, 552-567.

[52] Santapuri, S., Lowe, R. L., Bechtel, S. E. , Dapino, M. J. (2013). Thermodynamic modeling of fully coupled finite-deformation thermo-electro-magneto-mechanical behavior for multifunctional applications, *International Journal of Engineering Science*, **72**, 117–139.

[53] Shariff, M.H.B.M. (2000). Strain energy function for filled and unfilled rubberlike material, *Rubber Chem. Technol.*, **73**, 1-21.

[54] Shariff, M.H.B.M., Bustamante, R. (2015). On the independence of strain invariants of two preferred direction nonlinear elasticity, *International Journal of Engineering Science*, **97**, 18 - 25.

[55] Shariff, M.H.B.M. (2016). Anisotropic separable free energy functions for elastic and non-elastic solids. *Acta Mech.*, **227(11)**, 3213 - 3237.

[56] Shariff, M.H.B.M. , Bustamante, R. (2016). An anisotropic model for the Mullins effect in magnetoactive rubber-like materials. *Journal of Mechanics of Materials and Structures*, **11(5)**, 559 - 582.

[57] Shariff, M. H. B. M., Bustamante, R., Hossain, M. , Steinmann, P. (2017). A novel spectral formulation for transversely isotropic magneto-elasticity, *Mathematics and Mechanics of Solids*, **22**, 1158 - 1176.

[58] Shariff, M.H.B.M., (2017). The number of independent invariants of an n preferred direction anisotropic solid. *Math. Mech. Solids*, **22(10)**, 1989 - 1996.

[59] Shariff, M.H.B.M., Bustamante, R., Merodio, J. (2017). On the spectral analysis of residual stress in finite elasticity, *IMA J. Appl. Math.*, **82 (3)**, 656 -680.

[60] Shariff, M.H.B.M. (2017). Spectral derivatives in continuum mechanics.*Q. J. Mech. Appl. Mech.*, **70(4)**, 479 -476.

[61] Shariff, M.H.B.M. (2017). On the spectral constitutive modelling of transversely isotropic soft tissue: Physical invariants. *Int. J. Eng. Sci.*, **120** , 199 - 219.

[62] Shariff, M.H.B.M., Bustamante, R., Merodio, J. (2020). A nonlinear electro-elastic model with residual stresses and a preferred direction. *Mathematics and Mechanics of Solids*, **25 (3)**, 838 - 865.

[63] Shariff, M.H.B.M. , Merodio, J. (2020). Residually stressed two fibre solids: A spectral approach, *International Journal of Engineering Science*, **148**, https://doi.org/10.1016/j.ijengsci.2019.103205.

[64] Shariff, M.H.B.M., Bustamante, R., Merodio, J. (2020). A nonlinear constitutive model for a two preferred direction electro-elastic body with residual stresses. *International Journal of Non-Linear Mechanics*, **119**, 103352.

[65] Shariff, M.H.B.M., Bustamante, R., Merodio, J. (2020). A nonlinear spectral rate-dependent constitutive equation for electro-viscoelastic solids. *Z. Angew. Math. Phys.*, 71:126.

[66] Shariff, M.H.B.M. (2021). On the number of independent invariants for m unit vectors and n symmetric second order tensors. *Engineering Letters*, **29(2)** , 509 - 515.

[67] Spencer, A.J.M. (1971). Theory of invariants. In: A.C. Eringen Ed. Continuum Physics I, New York, Academic Press, 239 - 253.

[68] Vandiver, R., Goriely, A. (2009). Differential growth and residual stress in cylindrical elastic structures.*Philos.Trans.R.Soc. Lond.* **A367**: 3607-3630.

[69] Wan, X., Luo, L., Liu, Y., Leng, J. (2020). Direct Ink Writing Based 4D Printing of Materials and Their Applications, *Advanced Science*, **7**:2001000